Identification of keloid and surrounding healthy skin material parameters using Digital Image Correlation measurements in vivo

Aflah ELOUNEG

Thesis October 2018:
«Mechanical properties of the skin and uncertainties in biomechanics»
Funded by Region of Bourgogne-Franche-Comté (France)

Mechanical parameters identification of keloid and surrounding healthy skin using Digital Image Correlation measurements in vivo

Thesis October 2018:
«Mechanical properties of the skin and uncertainties in biomechanics»
Funded by Region of Bourgogne-Franche-Comté (France)

AEH team

Aflah ELOUNEG
Arnaud LEJEUNE
Jérôme CHAMBERT
Emmanuelle JACQUET

Mechanical parameters identification of keloid and surrounding healthy skin using Digital Image Correlation measurements in vivo

Thesis October 2018:
«Mechanical properties of the skin and uncertainties in biomechanics»
Funded by Region of Bourgogne-Franche-Comté (France)

Danas SUTULA

(Postdoc 2018)
FEniCS-based framework: Hyperelastic bi-material inverse identification

AEH team

Aflah ELOUNEG
Arnaud LEJEUNE
Jérôme CHAMBERT
Emmanuelle JACQUET

Mechanical parameters identification of keloid and surrounding healthy skin using Digital Image Correlation measurements in vivo

Thesis October 2018:
«Mechanical properties of the skin and uncertainties in biomechanics»
Funded by Region of Bourgogne-Franche-Comté (France)

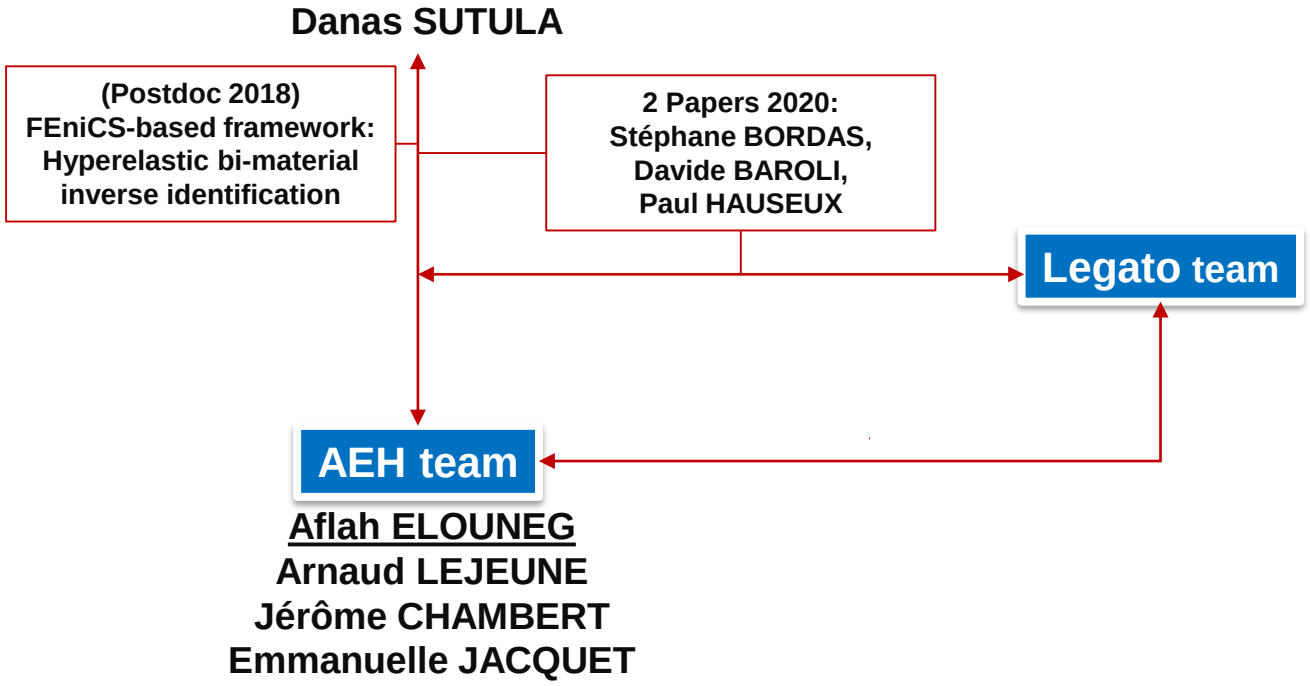

Mechanical parameters identification of keloid and surrounding healthy skin using Digital Image Correlation measurements in vivo

Thesis October 2018:
«Mechanical properties of the skin and uncertainties in biomechanics»
Funded by Region of Bourgogne-Franche-Comté (France)

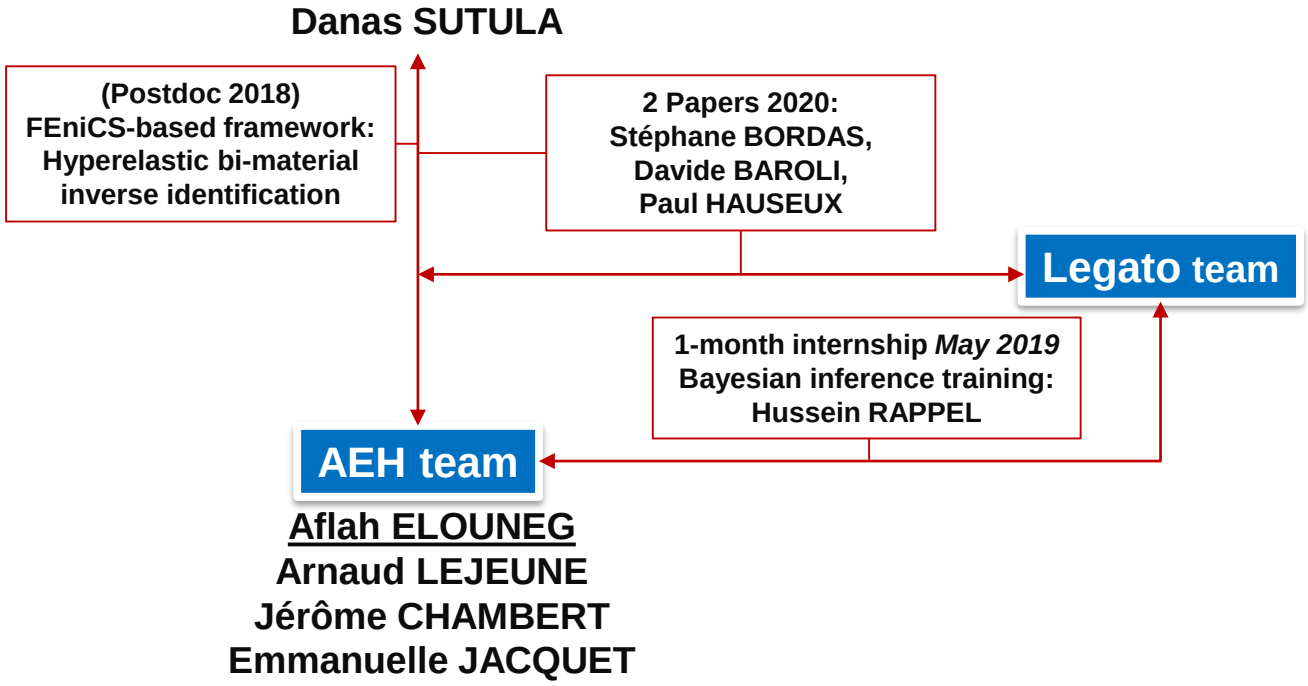

Mechanical parameters identification of keloid and surrounding healthy skin using Digital Image Correlation measurements in vivo

Thesis October 2018:
«Mechanical properties of the skin and uncertainties in biomechanics»
Funded by Region of Bourgogne-Franche-Comté (France)

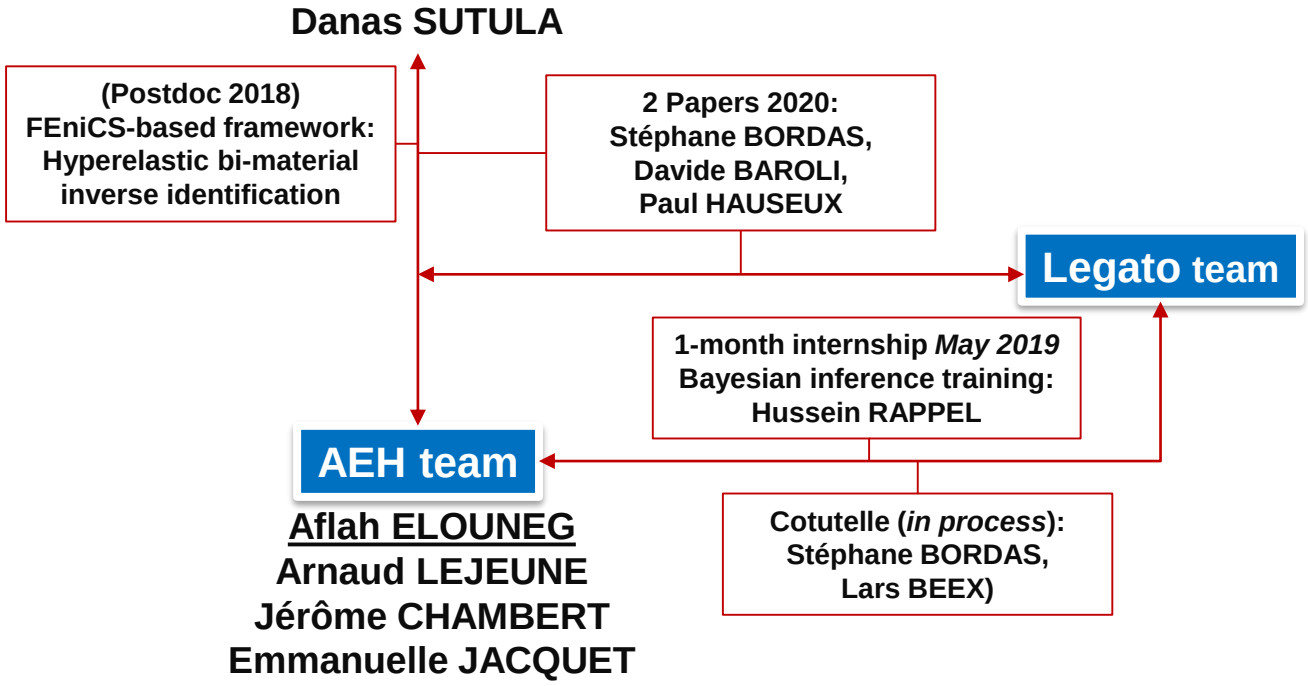

Mechanical parameters identification of keloid and surrounding healthy skin using Digital Image Correlation measurements in vivo

Thesis October 2018:
«Mechanical properties of the skin and uncertainties in biomechanics»
Funded by Region of Bourgogne-Franche-Comté (France)

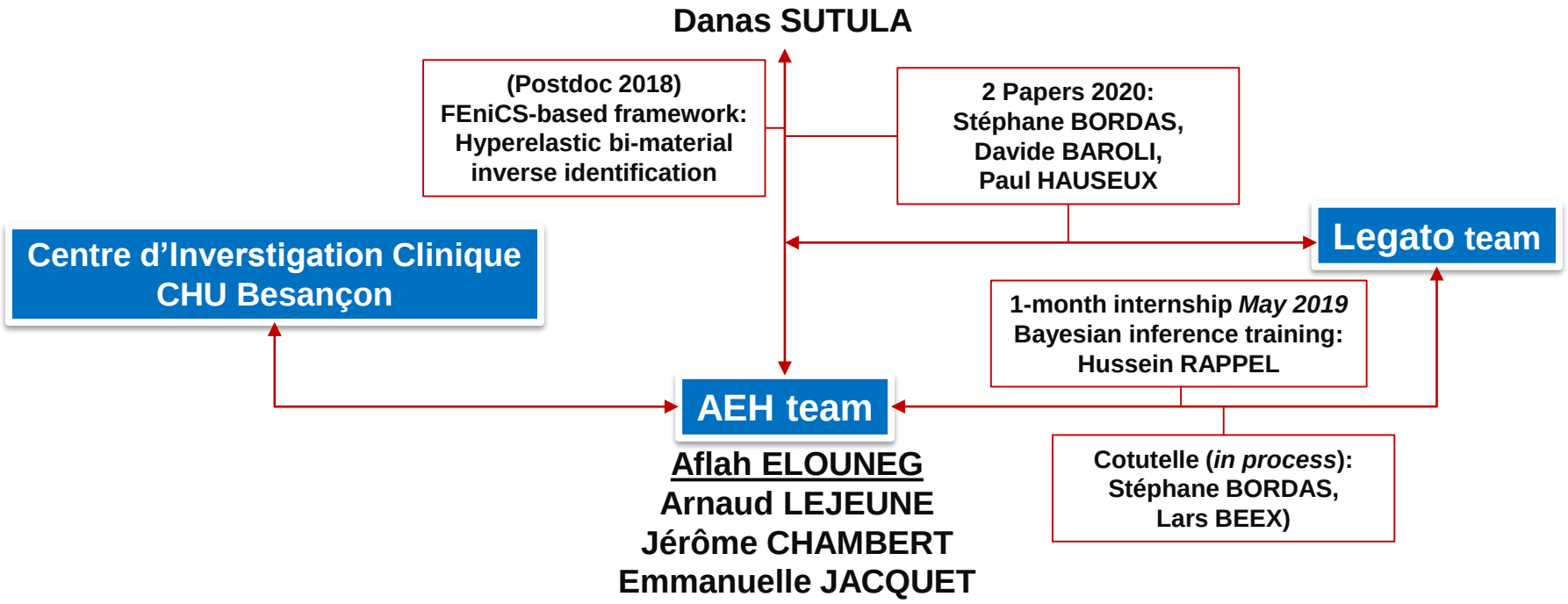

Mechanical parameters identification of keloid and surrounding healthy skin using Digital Image Correlation measurements in vivo

Thesis October 2018:
«Mechanical properties of the skin and uncertainties in biomechanics»
Funded by Region of Bourgogne-Franche-Comté (France)

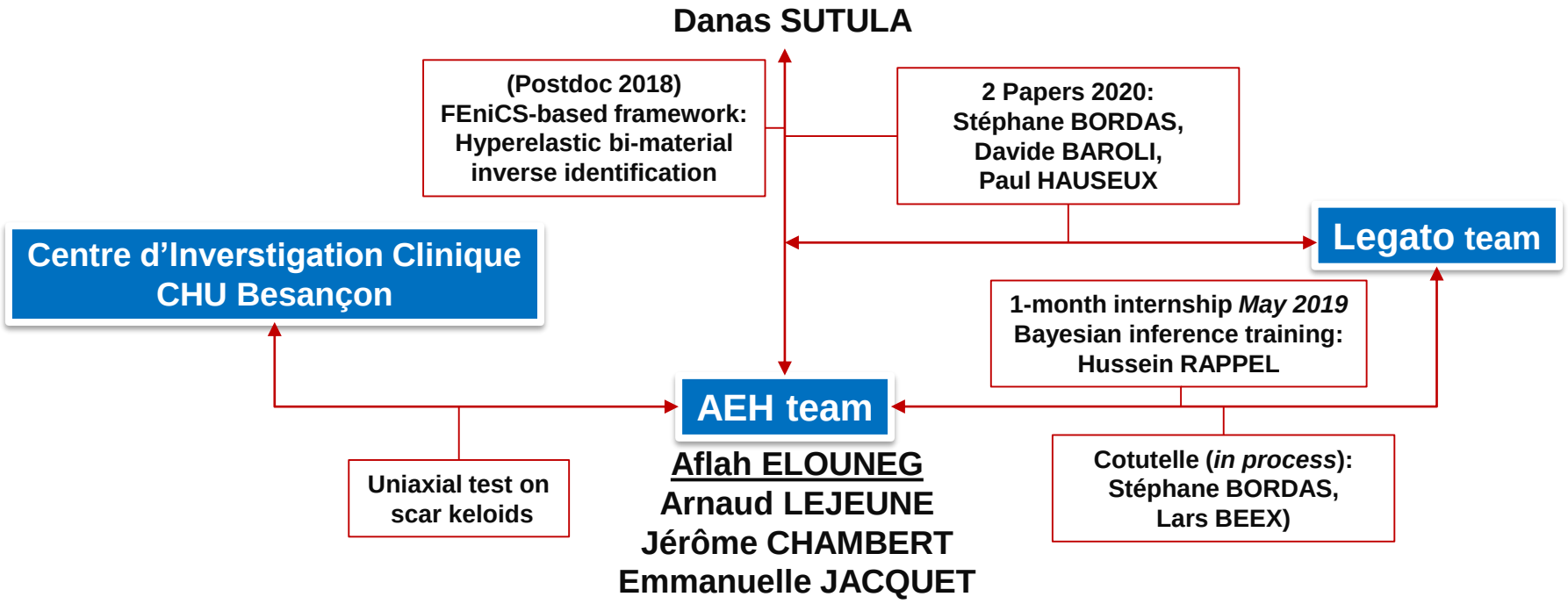

Mechanical parameters identification of keloid and surrounding healthy skin using Digital Image Correlation measurements in vivo

Thesis October 2018:
«Mechanical properties of the skin and uncertainties in biomechanics»
Funded by Region of Bourgogne-Franche-Comté (France)

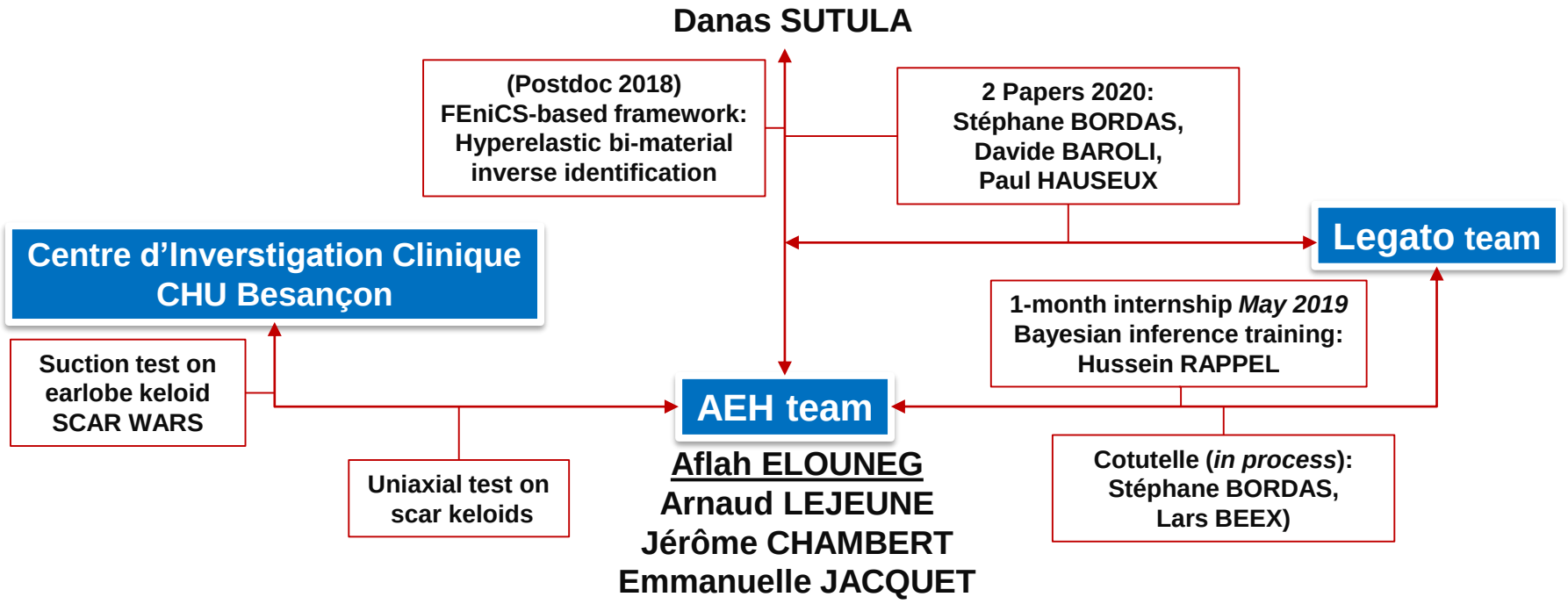

Mechanical parameters identification of keloid and surrounding healthy skin using Digital Image Correlation measurements in vivo

Thesis October 2018:
«Mechanical properties of the skin and uncertainties in biomechanics»
Funded by Region of Bourgogne-Franche-Comté (France)

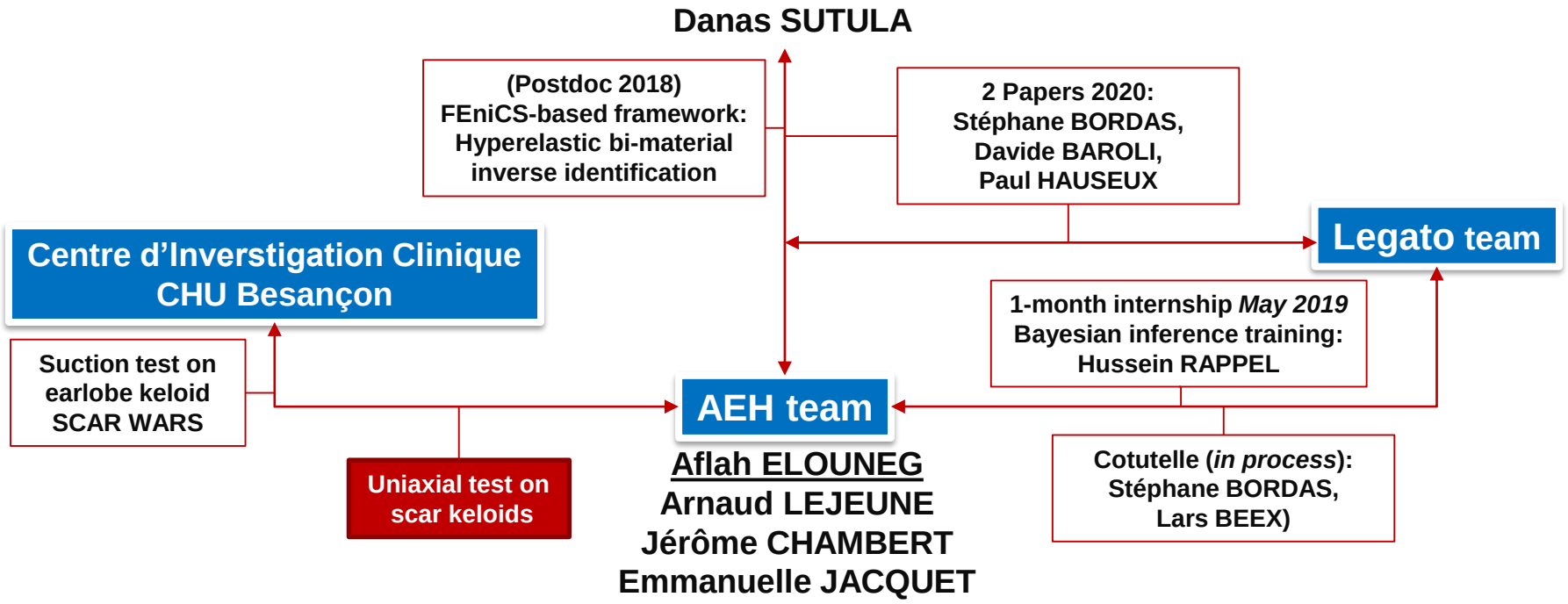

Mechanical parameters identification of keloid and surrounding healthy skin using Digital Image Correlation measurements in vivo

Context

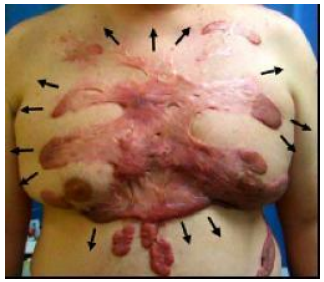

Keloid chest scar formation (Ogawa, 2008)

Keloid shoulder scar formation (Ogawa, 2008)

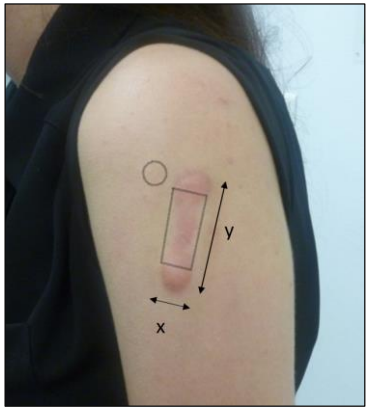

Butterfly-shaped keloid (x=15mm, y=47mm) (Chambert et al., 2019)

Keloid earlobe (healthline.com/health/keloids)

- **Benign tumor overgrowing beyond original wounds.**
- **The growth of a keloid is governed by many factors: biological, genetic and biomechanical.**

Aims:

- **Identify keloid material parameters (in vivo uniaxial and suction tests)**
- **Find the preferential directions of keloid growth.**
- **Establish specifications of a preventive clinical solution.**

Context

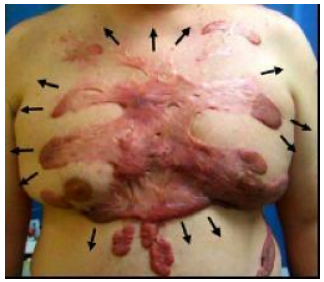

Keloid chest scar formation (Ogawa, 2008)

Keloid shoulder scar formation (Ogawa, 2008)

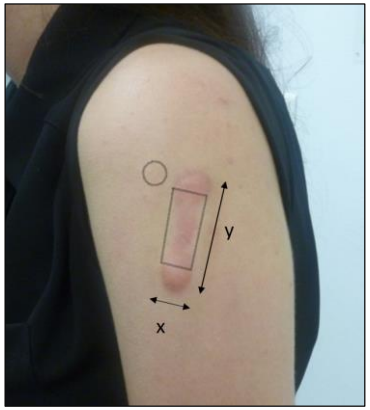

Butterfly-shaped keloid (x=15mm, y=47mm) (Chambert et al., 2019)

Keloid earlobe (healthline.com/health/keloids)

- **Benign tumor overgrowing beyond original wounds.**
- **The growth of a keloid is governed by many factors: biological, genetic and biomechanical.**

Aims:

- **Identify keloid material parameters (in vivo uniaxial and suction tests)**
- **Find the preferential directions of keloid growth.**
- **Establish specifications of a preventive clinical solution.**

Context

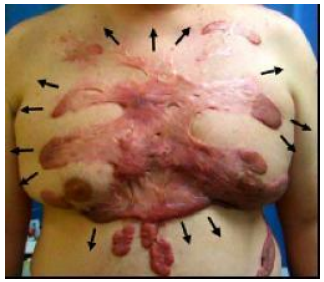

Keloid chest scar formation (Ogawa, 2008)

Keloid shoulder scar formation (Ogawa, 2008)

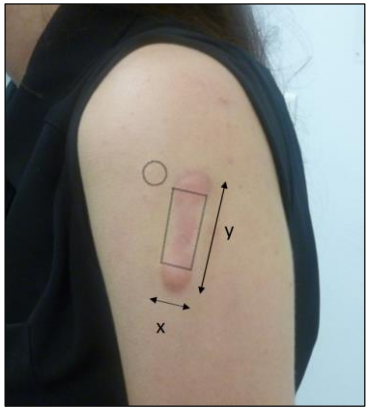

Butterfly-shaped keloid (x=15mm, y=47mm) (Chambert et al., 2019)

Keloid earlobe (healthline.com/health/keloids)

- Benign tumor overgrowing beyond original wounds.
- The growth of a keloid is governed by many factors: biological, genetic and biomechanical.

Aims:

- Identify keloid material parameters (in vivo uniaxial and suction tests)
- Find the preferential directions of keloid growth.
- Establish specifications of a preventive clinical solution.

Context

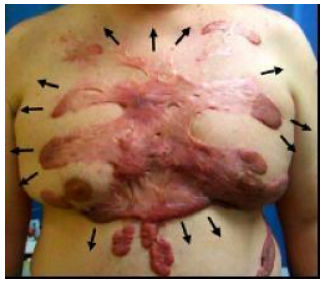

Keloid chest scar formation (Ogawa, 2008)

Keloid shoulder scar formation (Ogawa, 2008)

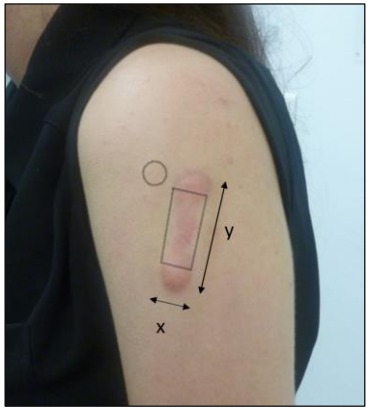

Butterfly-shaped keloid (x=15mm, y=47mm) (Chambert et al., 2019)

Keloid earlobe (healthline.com/health/keloids)

- Benign tumor overgrowing beyond original wounds.
- The growth of a keloid is governed by many factors: biological, genetic and biomechanical.

Aims:

- Identify keloid material parameters (in vivo uniaxial and suction tests)
- Find the preferential directions of keloid growth.
- Establish specifications of a preventive clinical solution.

Context

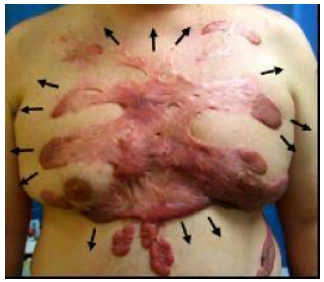

Keloid chest scar formation (Ogawa, 2008)

Keloid shoulder scar formation (Ogawa, 2008)

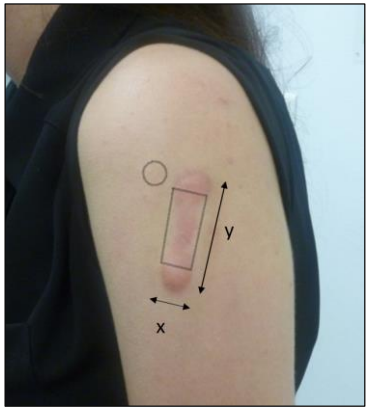

Butterfly-shaped keloid (x=15mm, y=47mm) (Chambert et al., 2019)

Keloid earlobe (healthline.com/health/keloids)

- Benign tumor overgrowing beyond original wounds.
- The growth of a keloid is governed by many factors: biological, genetic and biomechanical.

Aims:

- Identify keloid material parameters (in vivo uniaxial and suction tests)
- Find the preferential directions of keloid growth.
- Establish specifications of a preventive clinical solution.

Outlines:

- Uniaxial tensile test on bi-material soft tissues
- FEniCS-based framework of the inverse identification
- Sensitivity analysis (noisy *in silico* data)
- Application to keloid scar surrounded by healthy skin
- Conclusion and perspectives

Uniaxial tensile test on bi-material soft tissues

Experimental data: Force-displacement curve (FD)

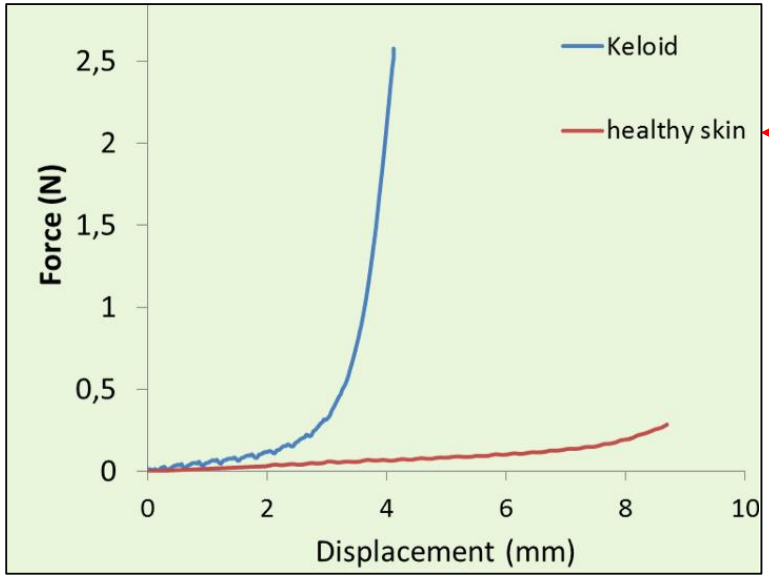

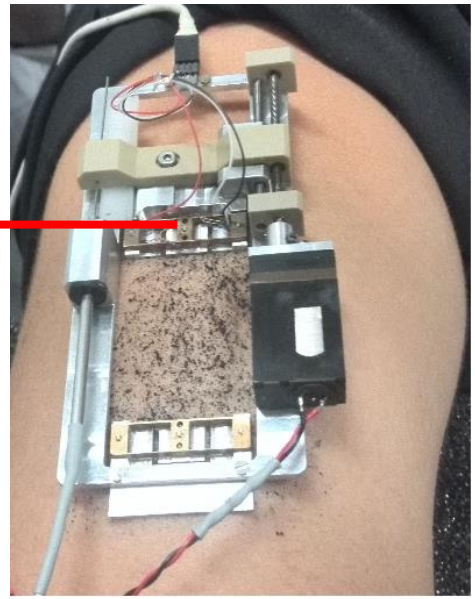

DIC Speckle pattern (Jacquet et al. 2017)

Uniaxial tensile test on bi-material soft tissues

Experimental data: Digital Image Correlation (DIC)

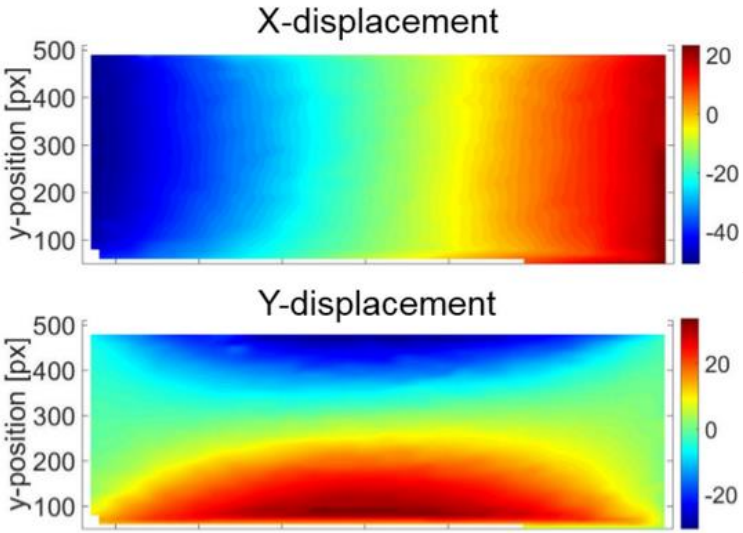

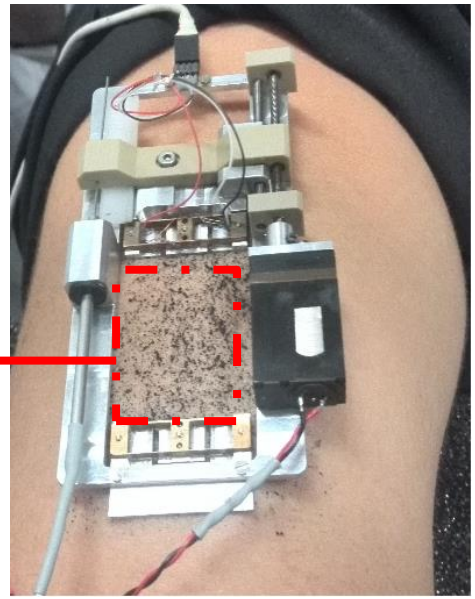

DIC Speckle pattern (Jacquet et al. 2017)

Mechanical parameters identification of keloid and surrounding healthy skin using Digital Image Correlation measurements in vivo

Uniaxial tensile test on bi-material soft tissues

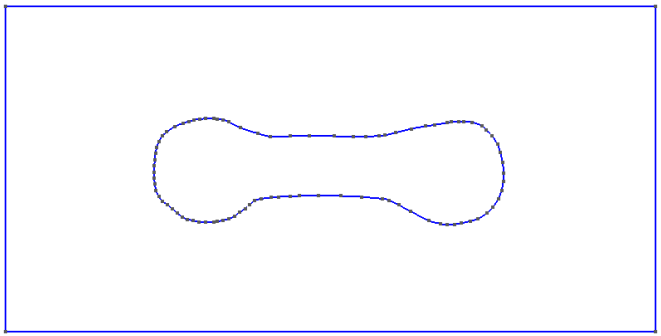

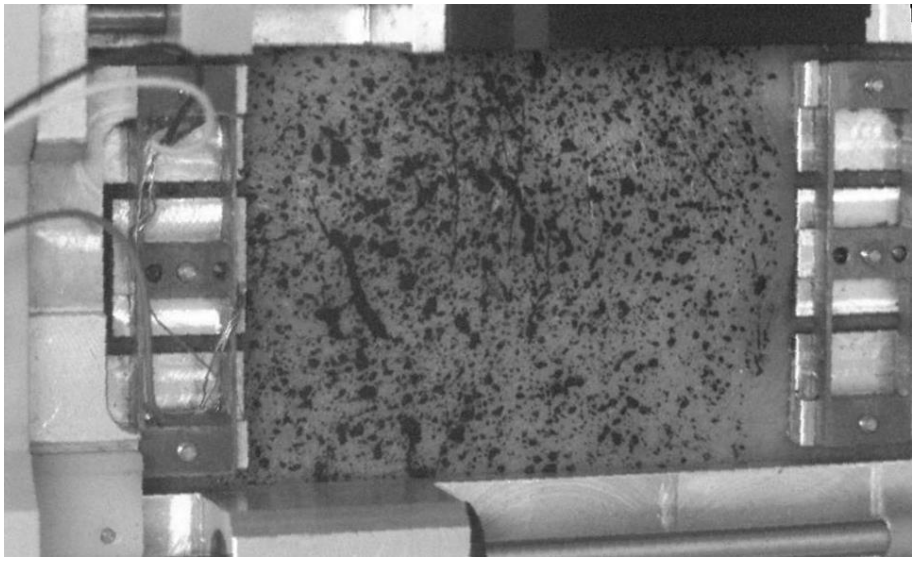

Uniaxial tensile test on bi-material soft tissues

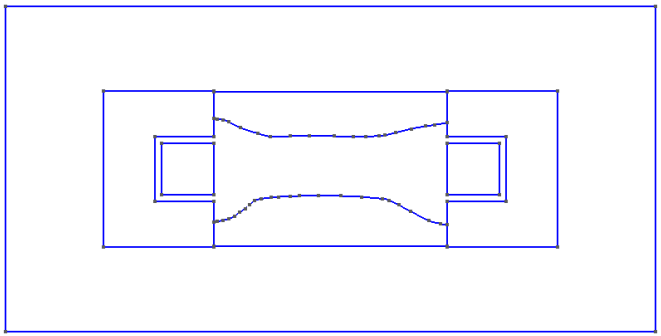

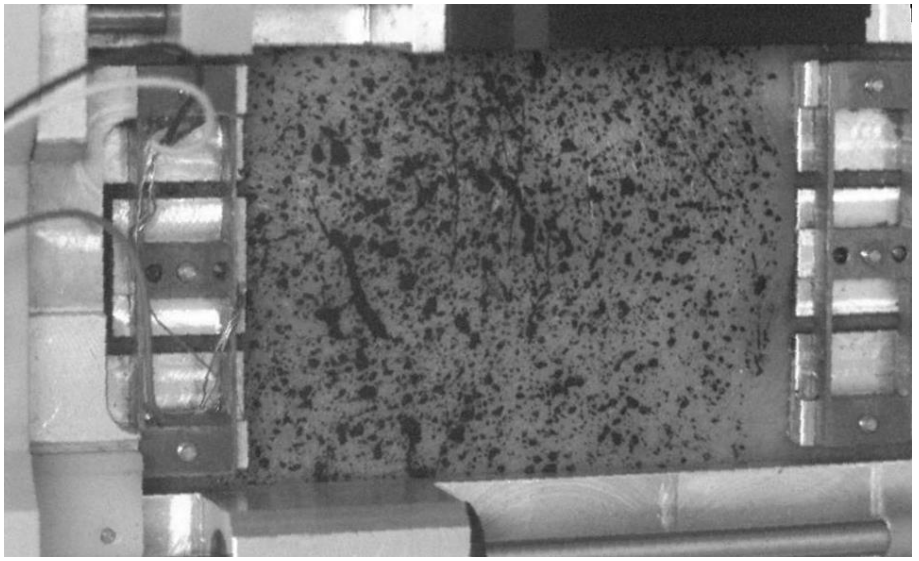

Uniaxial tensile test on bi-material soft tissues

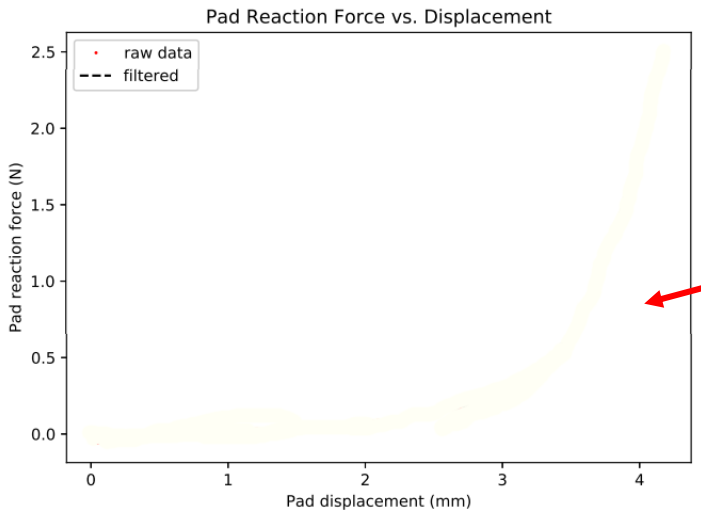

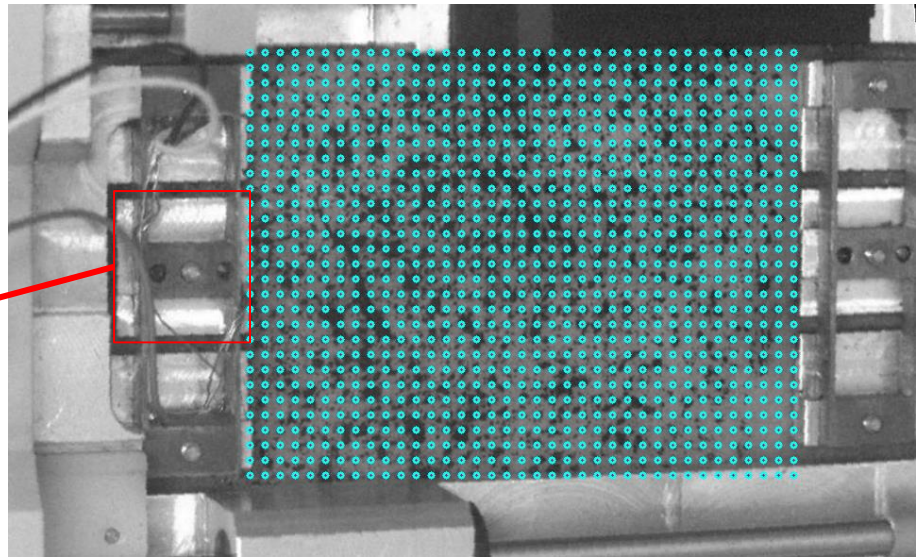

Experimental data: **Force-Displacement** and **DIC (Digital Image Correlation)**

Uniaxial tensile test on bi-material soft tissues

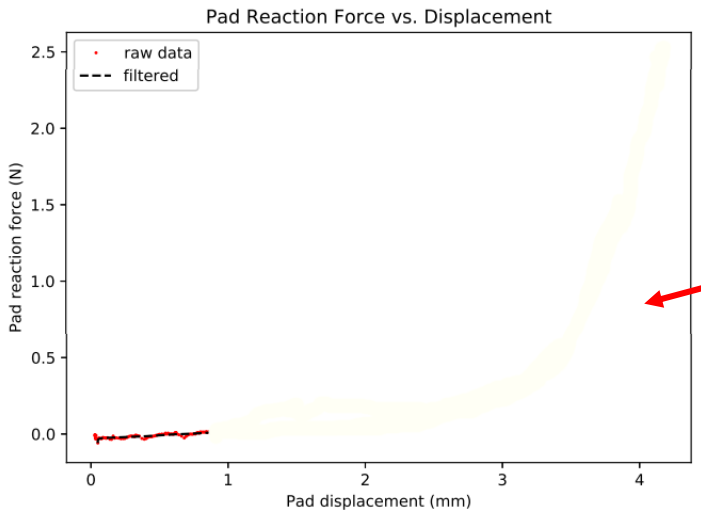

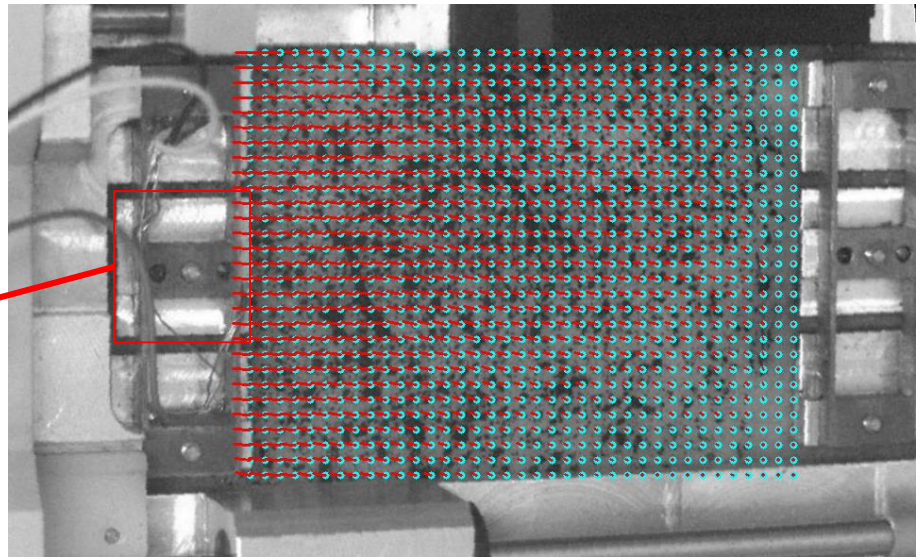

Experimental data: **Force-Displacement** and **DIC (Digital Image Correlation)**

Uniaxial tensile test on bi-material soft tissues

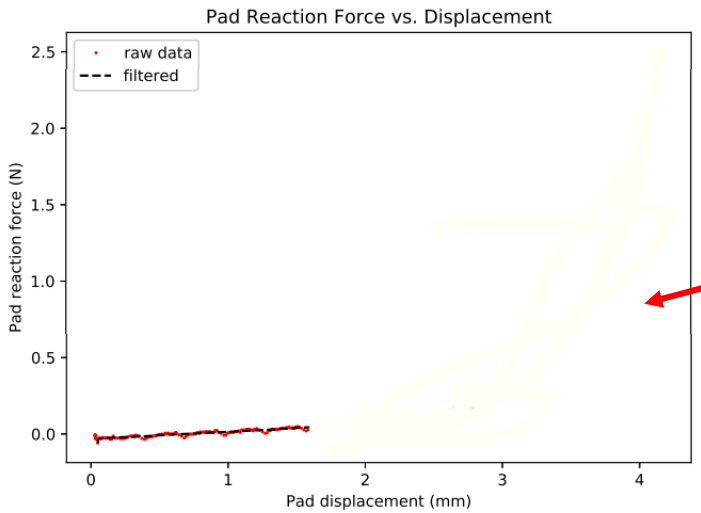

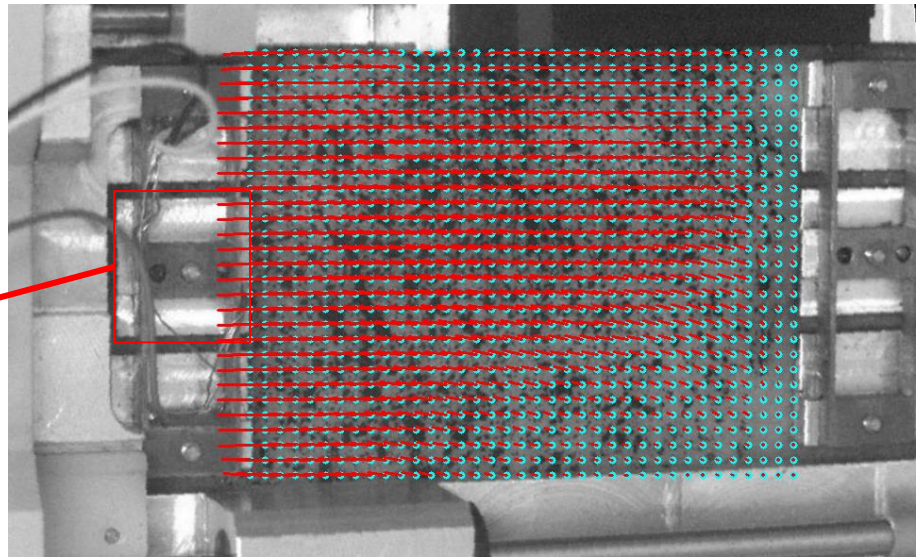

Experimental data: **Force-Displacement** and **DIC (Digital Image Correlation)**

Uniaxial tensile test on bi-material soft tissues

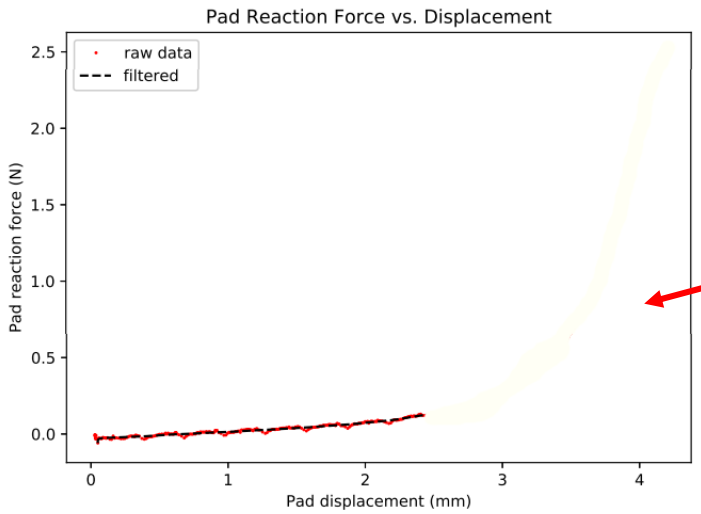

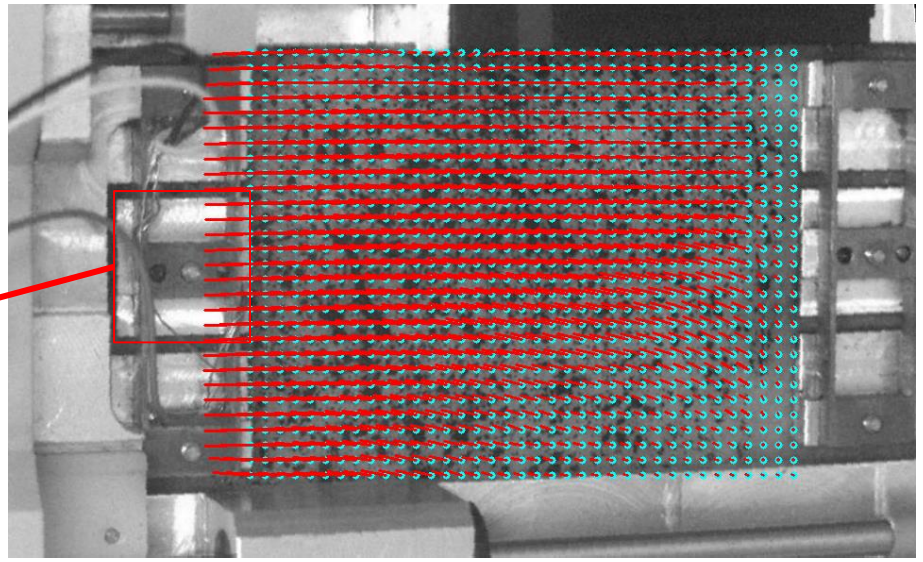

Experimental data: **Force-Displacement** and **DIC (Digital Image Correlation)**

Uniaxial tensile test on bi-material soft tissues

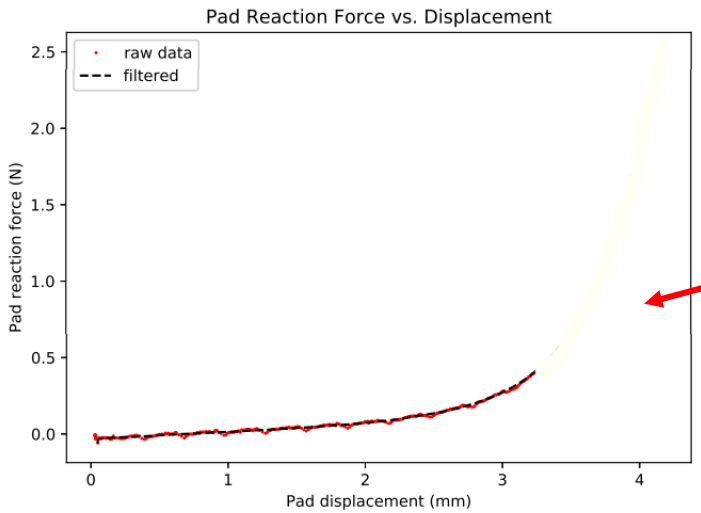

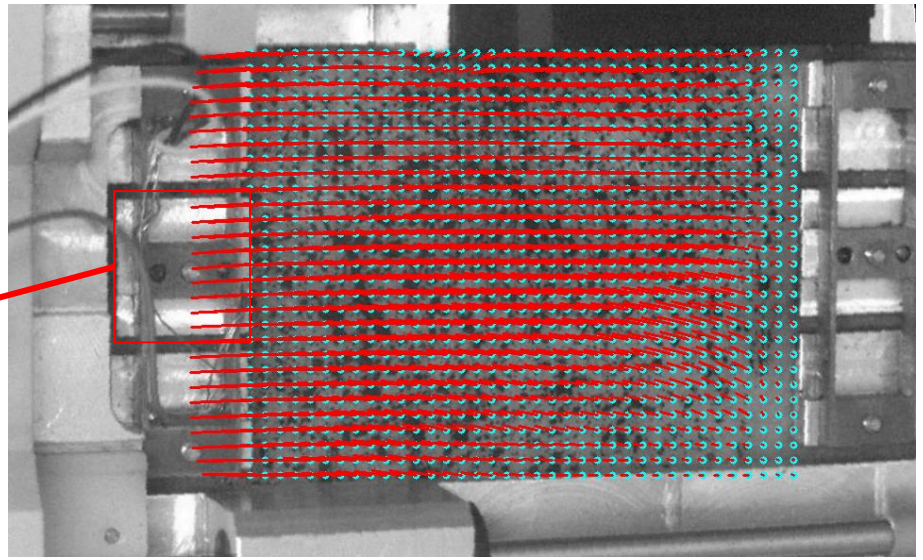

Experimental data: **Force-Displacement** and **DIC (Digital Image Correlation)**

Uniaxial tensile test on bi-material soft tissues

99 FD-DIC snapshots

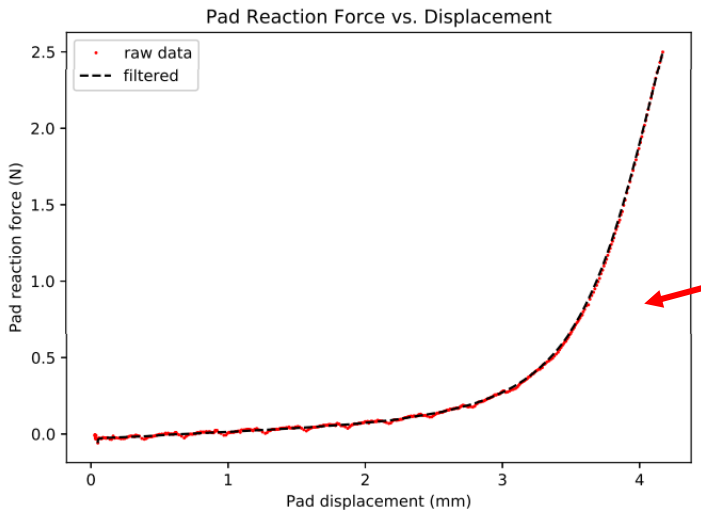

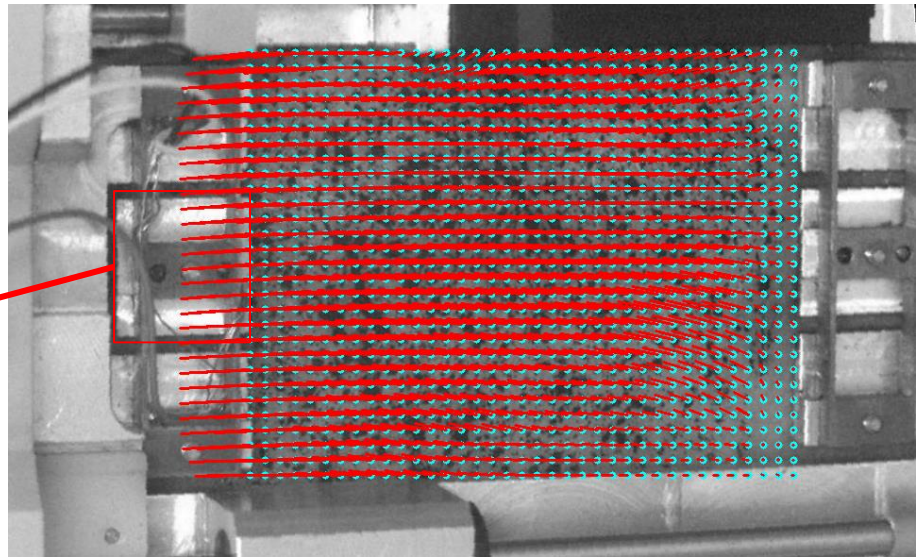

Experimental data: **Force-Displacement** and **DIC (Digital Image Correlation)**

FEniCS-based framework of the inverse identification

FEniCS-based framework of the inverse identification

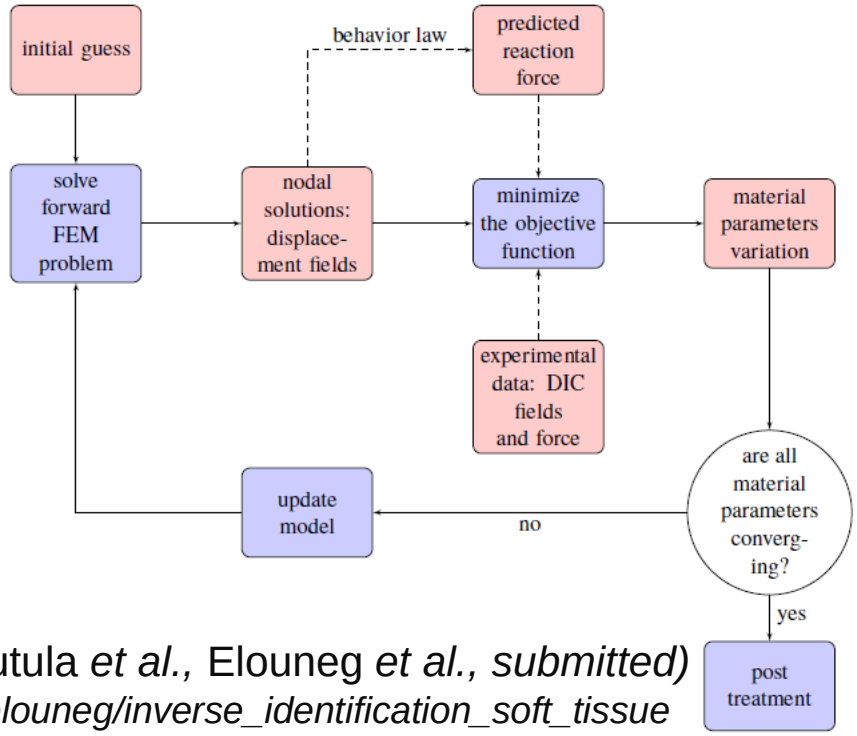

FEMU flow chart (Sutula *et al.*, Elouneg *et al., submitted)*
https://github.com/aflahelouneg/inverse_identification_soft_tissue

FEniCS-based framework of the inverse identification

FE nonlinear model
- Bi-material
- Hyperlastic behavior: *Gent*
- *2D geometry*

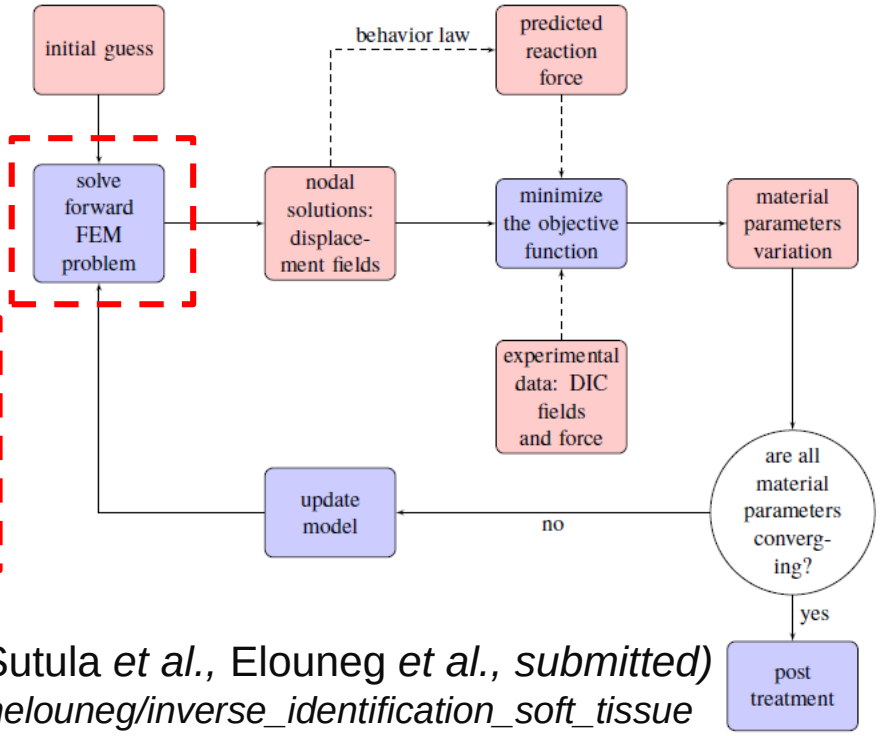

FEMU flow chart (Sutula *et al.*, Elouneg *et al., submitted)*

https://github.com/aflahelouneg/inverse_identification_soft_tissue

FEniCS-based framework of the inverse identification

Assumptions:

- Both keloid and skin have the same hyperelastic constitutive law, but different parameters.

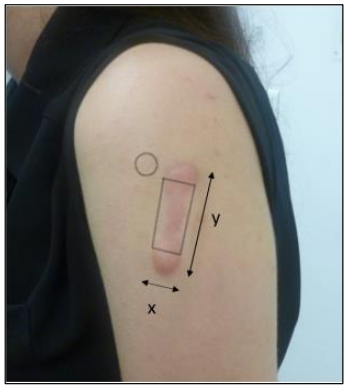

FEniCS-based framework of the inverse identification

FENICS PROJECT

Assumptions:

- Both keloid and skin have the same hyperelastic constitutive law, but different parameters.
- Plane strain conditions are made for the whole 2D structure considering sub-cutaneous links (unlike ex vivo).

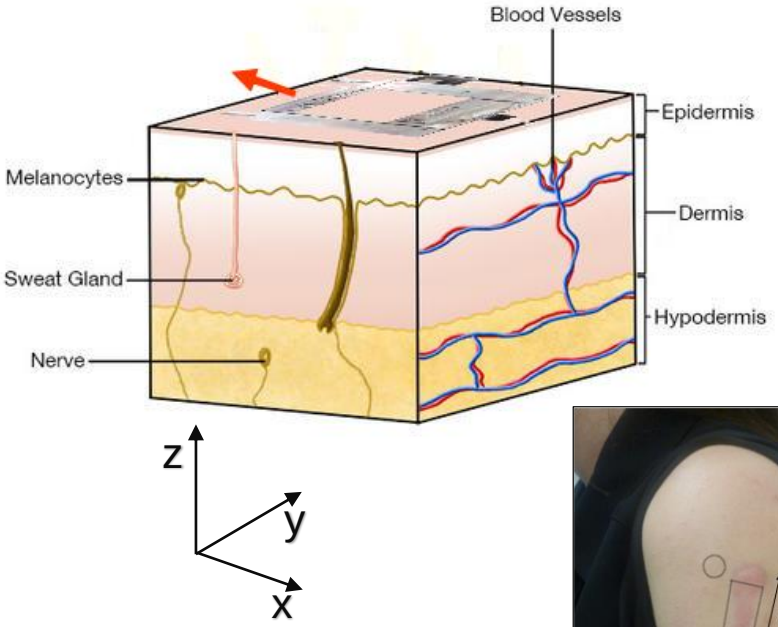

$$\varepsilon_{xz} = \varepsilon_{yz} = \varepsilon_{zz} = 0$$

[Krueger *et al.* 2002]

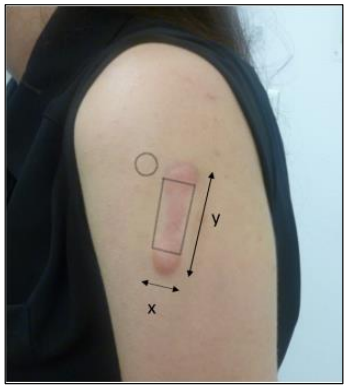

FEniCS-based framework of the inverse identification

Hyperelastic behavior law

Gent **model**

$$\psi(\mu, J_m, I_1) = -\frac{\mu}{2} J_m \, ln\left(1 - \frac{I_1 - 3}{J_m}\right)$$

$$I_1 = Tr\left(FF^T\right) = \lambda_1^2 + \lambda_2^2 + \lambda_3^2$$

Stress/strain curve (Puglisi 2015)

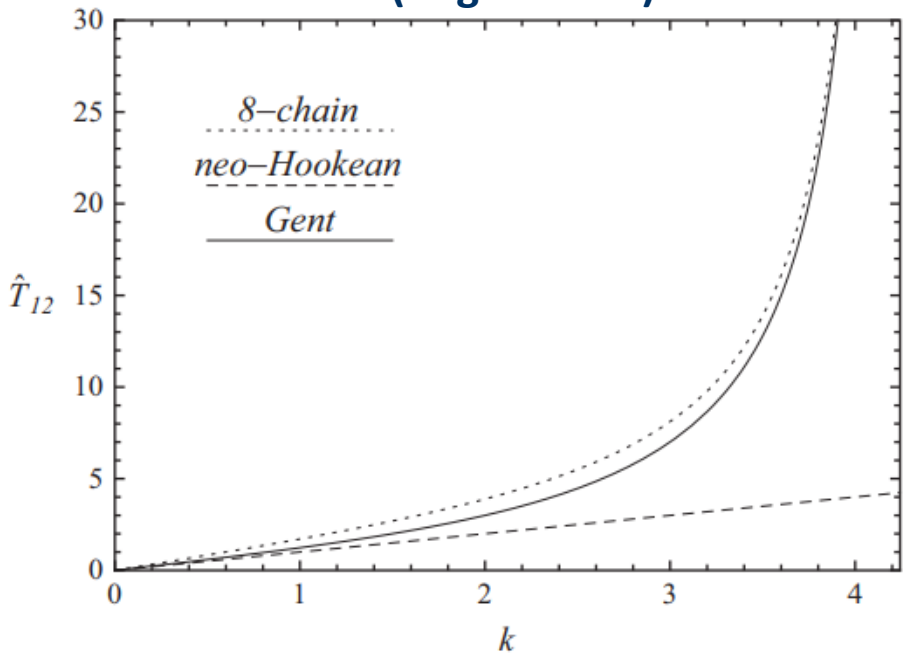

FEniCS-based framework of the inverse identification

Hyperelastic behavior law

***Gent* model**

$$\psi(\mu, J_m, I_1) = -\frac{\mu}{2} J_m \, ln\left(1 - \frac{I_1 - 3}{J_m}\right)$$

$$I_1 = Tr(FF^T) = \lambda_1^2 + \lambda_2^2 + \lambda_3^2$$

Incompressible material:

$$J_m < \lambda_1^2 + \frac{2}{\lambda_1} - 3$$

Stress/strain curve (Puglisi 2015)

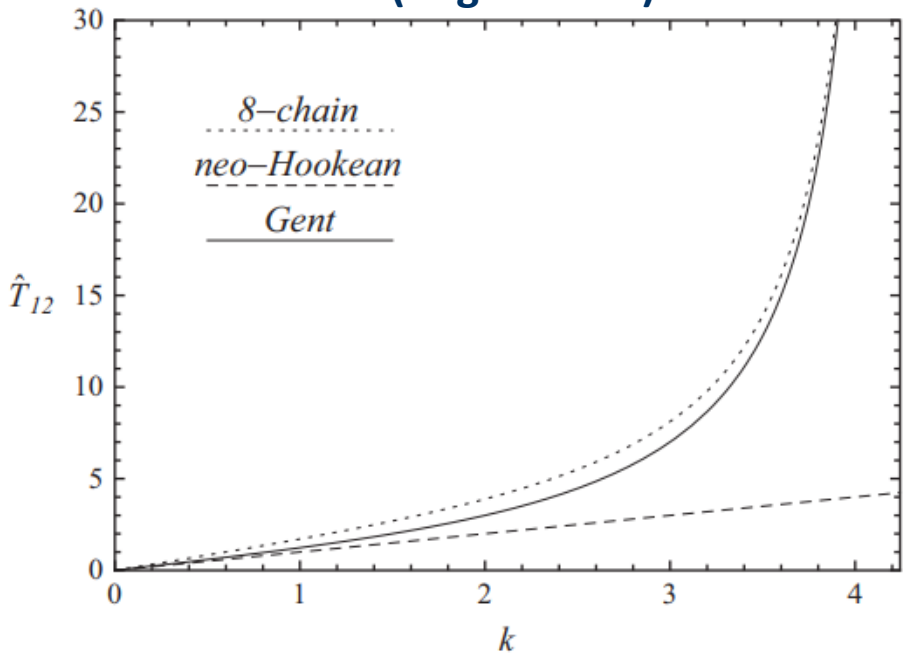

FEniCS-based framework of the inverse identification

$$\boldsymbol{\theta} = \{\boldsymbol{\theta}_{keloid}, \boldsymbol{\theta}_{healthy-skin}\}$$

$$\boldsymbol{\theta} = \arg_{min} J(\theta, \lambda)$$

$$J(\theta,\lambda) = \frac{1}{N_{frames}} \sum_{k=1}^{N_{frames}} \left[\int_{\Omega_{msr}} \frac{1}{\boldsymbol{\alpha^2}} \left\| \boldsymbol{u}_{fem}^{(k)}(\theta) - \boldsymbol{u}_{msr}^{(k)} \right\|^2 dx + \boldsymbol{\lambda} \frac{1}{\boldsymbol{\beta}} \left(F_{fem}^{(k)} - F_{msr}^{(k)} \right) \right]$$

Constant weights

$$\alpha = \max_{k=0,1,\ldots,N_{frames}} \left\| \boldsymbol{u}_{msr}^{(k)} \right\|_{\Omega_{msr}}$$

$$\beta = \max_{k=0,1,\ldots,N_{frames}} \left| F_{msr}^{(k)} \right|$$

λ: Lagrange multiplier

FEniCS-based framework of the inverse identification

$$\boldsymbol{\theta} = \{\boldsymbol{\theta}_{keloid}, \boldsymbol{\theta}_{healthy-skin}\}$$

$$\boldsymbol{\theta} = \arg_{min} J(\theta, \lambda)$$

$$J(\theta,\lambda) = \frac{1}{N_{frames}} \sum_{k=1}^{N_{frames}} \left[\int_{\Omega_{msr}} \frac{1}{\alpha^2} \left\| \boldsymbol{u}_{fem}^{(k)}(\theta) - \boldsymbol{u}_{msr}^{(k)} \right\|^2 dx + \lambda \frac{1}{\beta} \left(F_{fem}^{(k)} - F_{msr}^{(k)} \right) \right]$$

FEniCS-based framework of the inverse identification

$$\boldsymbol{\theta} = \{\boldsymbol{\theta}_{keloid}, \boldsymbol{\theta}_{healthy-skin}\}$$

$$\boldsymbol{\theta} = \arg_{min} J(\theta, \lambda)$$

$$J(\theta,\lambda) = \frac{1}{N_{frames}} \sum_{k=1}^{N_{frames}} \left[\int_{\Omega_{msr}} \frac{1}{\alpha^2} \left\| \boldsymbol{u}_{fem}^{(k)}(\theta) - \boldsymbol{u}_{msr}^{(k)} \right\|^2 dx + \lambda \frac{1}{\beta} \left(F_{fem}^{(k)} - F_{msr}^{(k)} \right) \right]$$

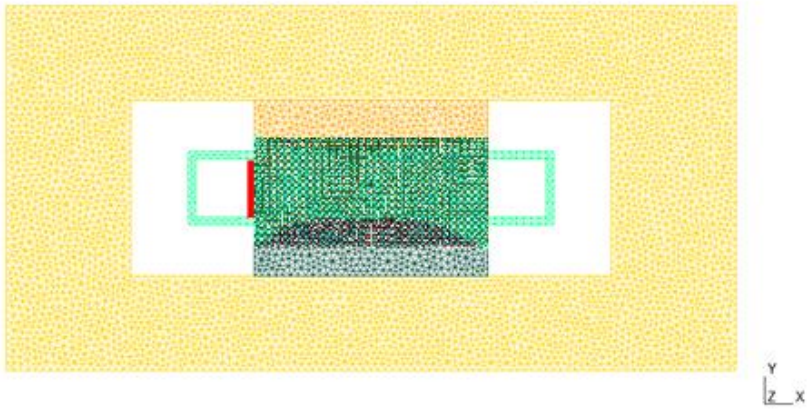

Mechanical parameters identification of keloid and surrounding healthy skin using Digital Image Correlation measurements in vivo

FEniCS-based framework of the inverse identification

$$\boldsymbol{\theta} = \{\boldsymbol{\theta}_{keloid}, \boldsymbol{\theta}_{healthy-skin}\}$$

$$\boldsymbol{\theta} = \arg_{min} J(\theta, \lambda)$$

$$J(\theta,\lambda) = \frac{1}{N_{frames}} \sum_{k=1}^{N_{frames}} \left[\int_{\Omega_{msr}} \frac{1}{\alpha^2} \left\| \boldsymbol{u}_{fem}^{(k)}(\theta) - \boldsymbol{u}_{msr}^{(k)} \right\|^2 dx + \lambda \frac{1}{\beta} \left(F_{fem}^{(k)} - F_{msr}^{(k)} \right) \right]$$

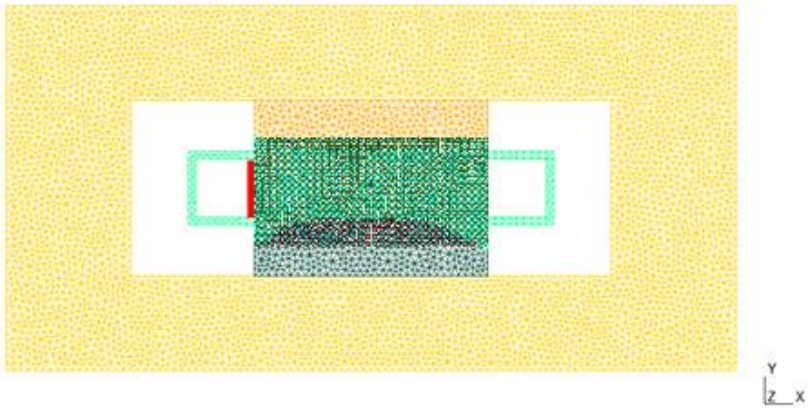

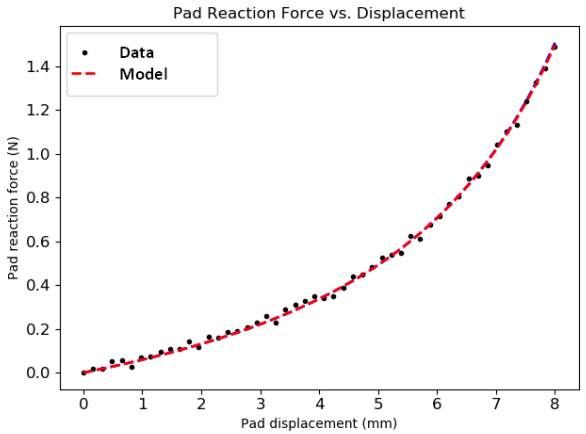

Mechanical parameters identification of keloid and surrounding healthy skin using Digital Image Correlation measurements in vivo

Validation using dummy data

Material parameters (arbitrary)

Validation using dummy data

Gent model

$$\psi(\mu, j_m, I_1) = -\frac{\mu}{2}\left[j_m \, ln\left(1 - \frac{I_1 - 3}{j_m}\right) + 2ln(J)\right]$$

$$I_1 = Tr(FF^T)$$

Validation using dummy data

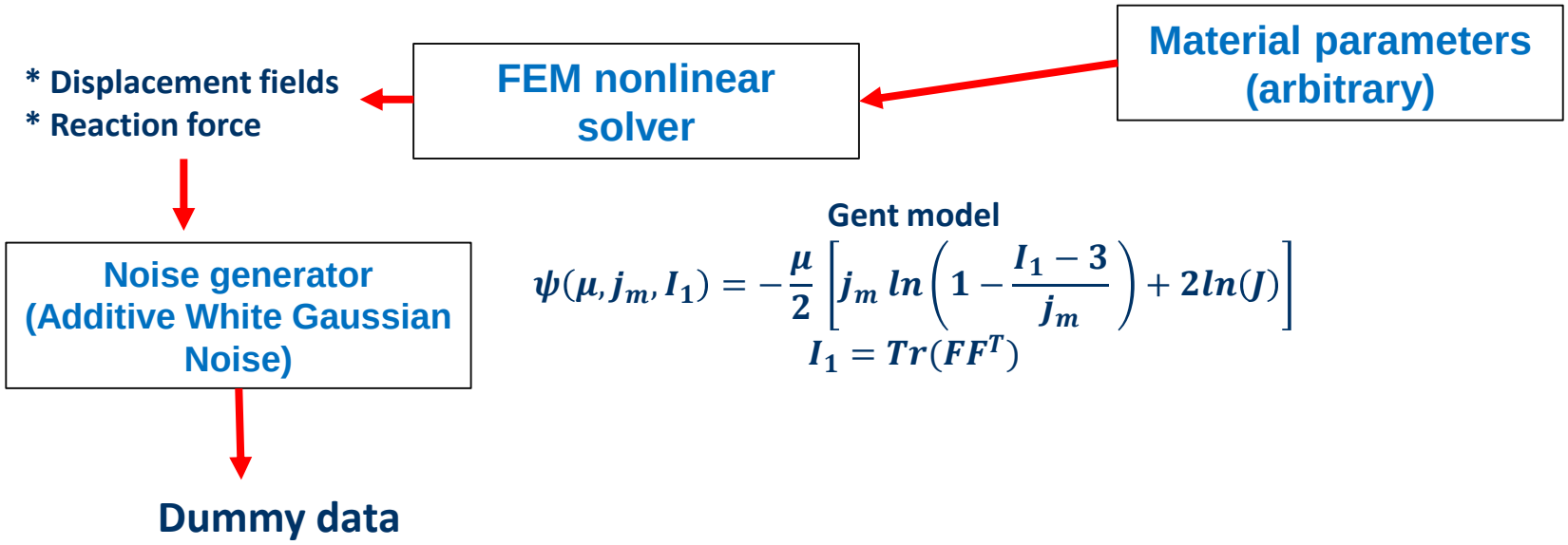

Gent model

$$\psi(\mu, j_m, I_1) = -\frac{\mu}{2}\left[j_m \, ln\left(1 - \frac{I_1 - 3}{j_m}\right) + 2ln(J)\right]$$

$$I_1 = Tr(FF^T)$$

Validation using dummy data

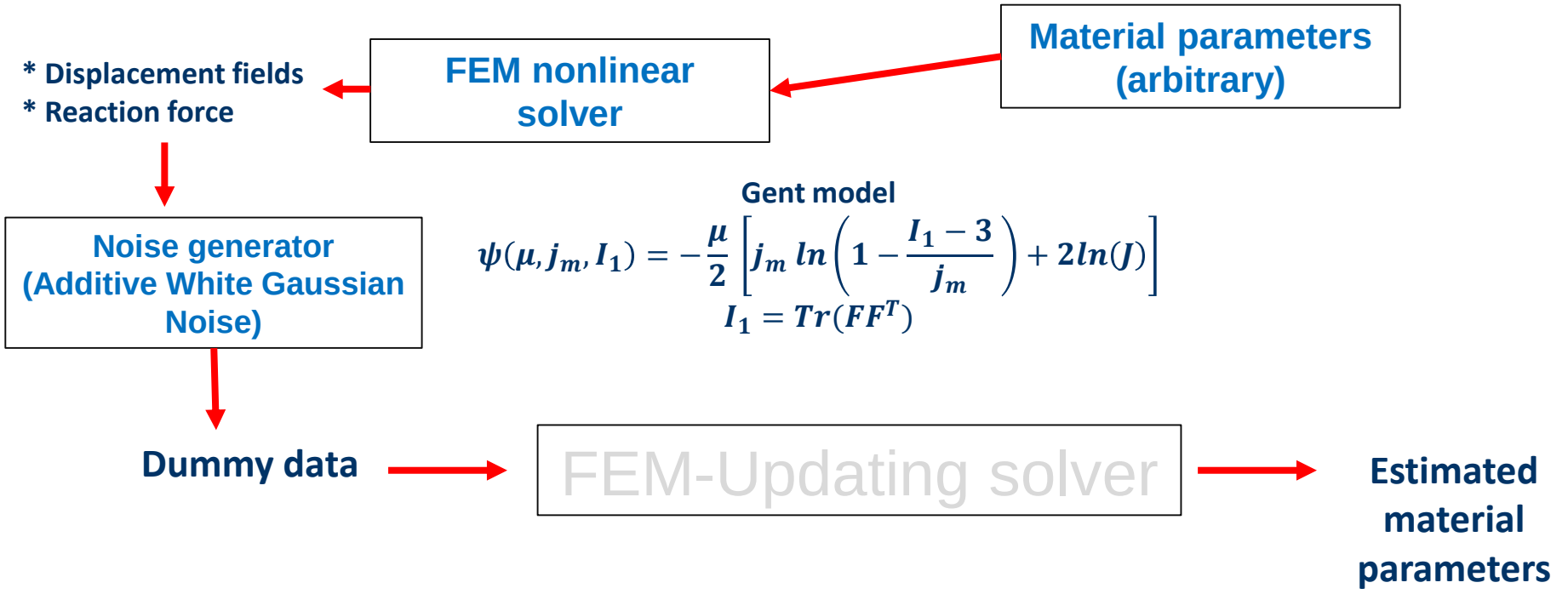

Validation using dummy data

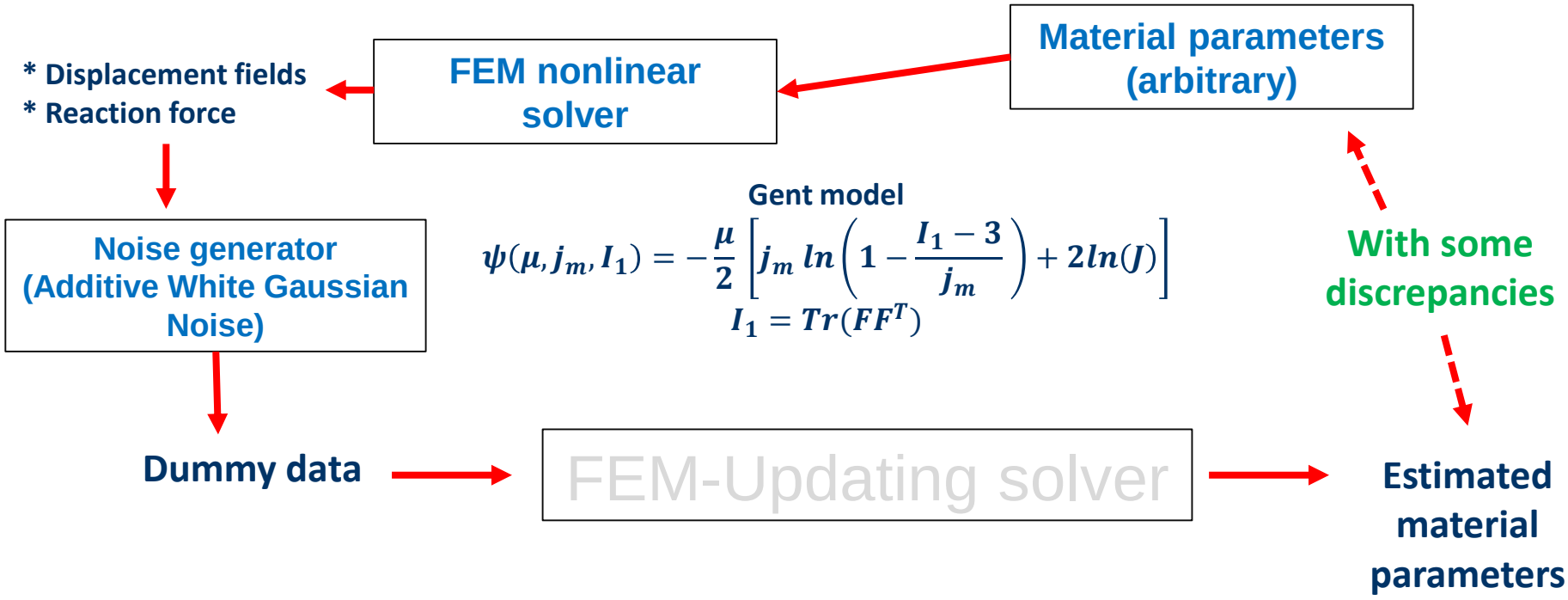

Sensitivity analysis

- **Discretization error.**
- **Measurement noises standard deviation.**
- **Number of DIC frames.**

Sensitivity analysis

- **Discretization error.**
- **Measurement noises standard deviation.**
- **Number of DIC frames.**

Quantification of parameter identification discrepancy with respect to discretization error

$$\varepsilon_i = \frac{\left|\theta_i - \theta_{i_{ref}}\right|}{\left|\theta_{i_{ref}}\right|}; 1 \leq i \leq 4$$

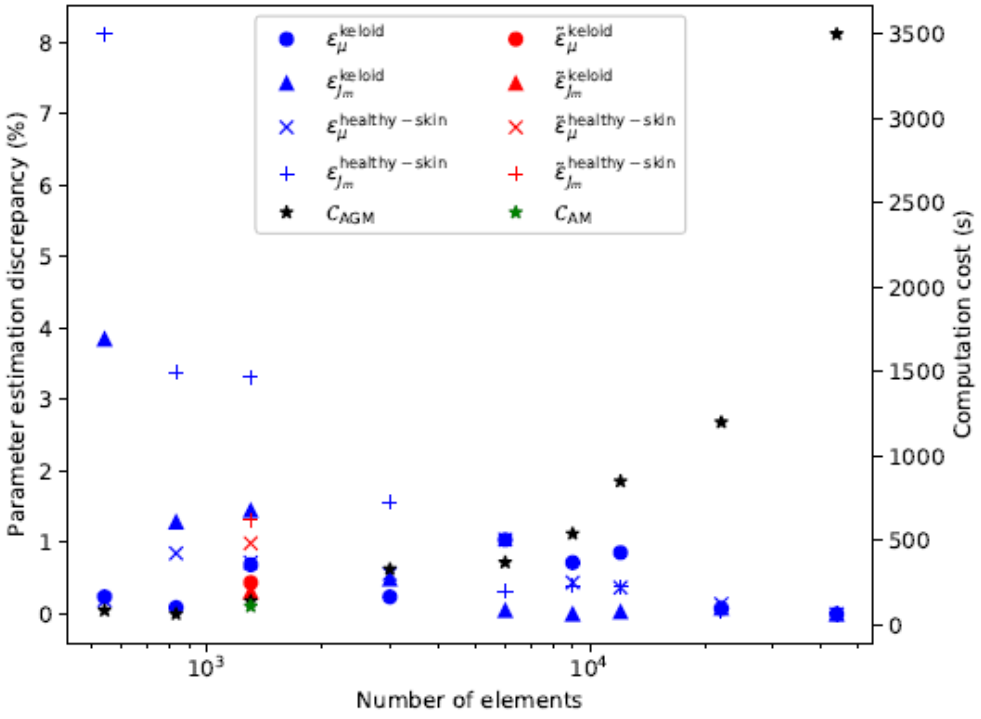

Sensitivity analysis

- Discretization error.
- **Measurement noises standard deviation.**
- Number of DIC frames.

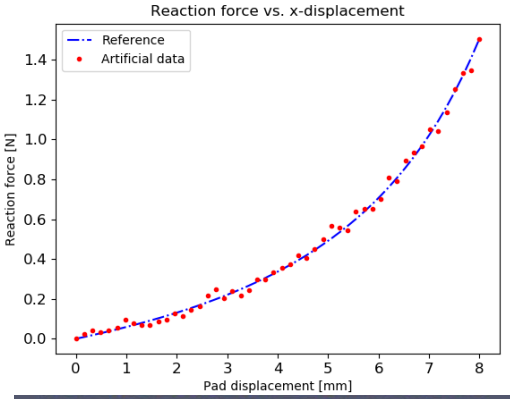

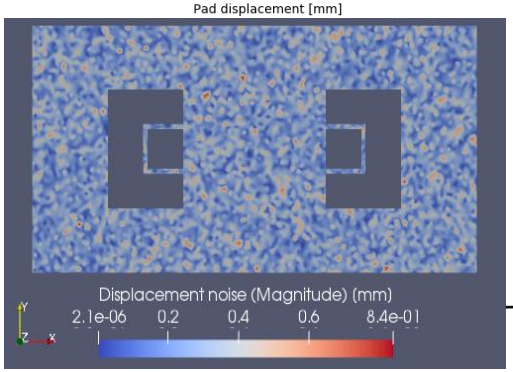

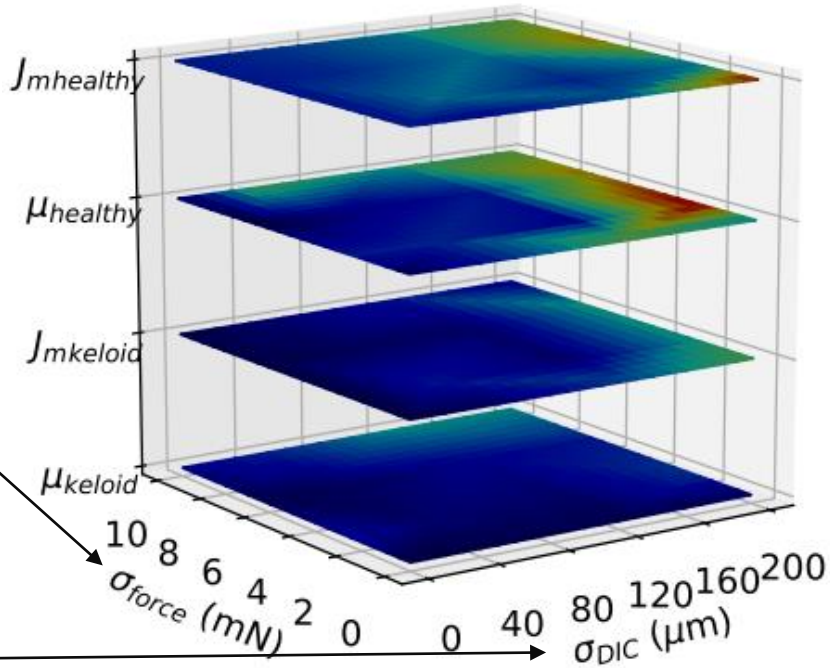

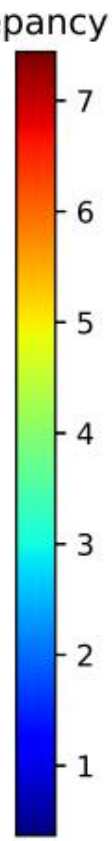

Adaptive mesh 1300 cells

Mechanical parameters identification of keloid and surrounding healthy skin using Digital Image Correlation measurements in vivo

Sensitivity analysis

- Discretization error.
- Measurement noises standard deviation.
- Number of DIC frames.

$$\sigma_{DIC_{max}} = 160\ \mu m$$

$$\sigma_{force_{max}} = 10\ mN$$

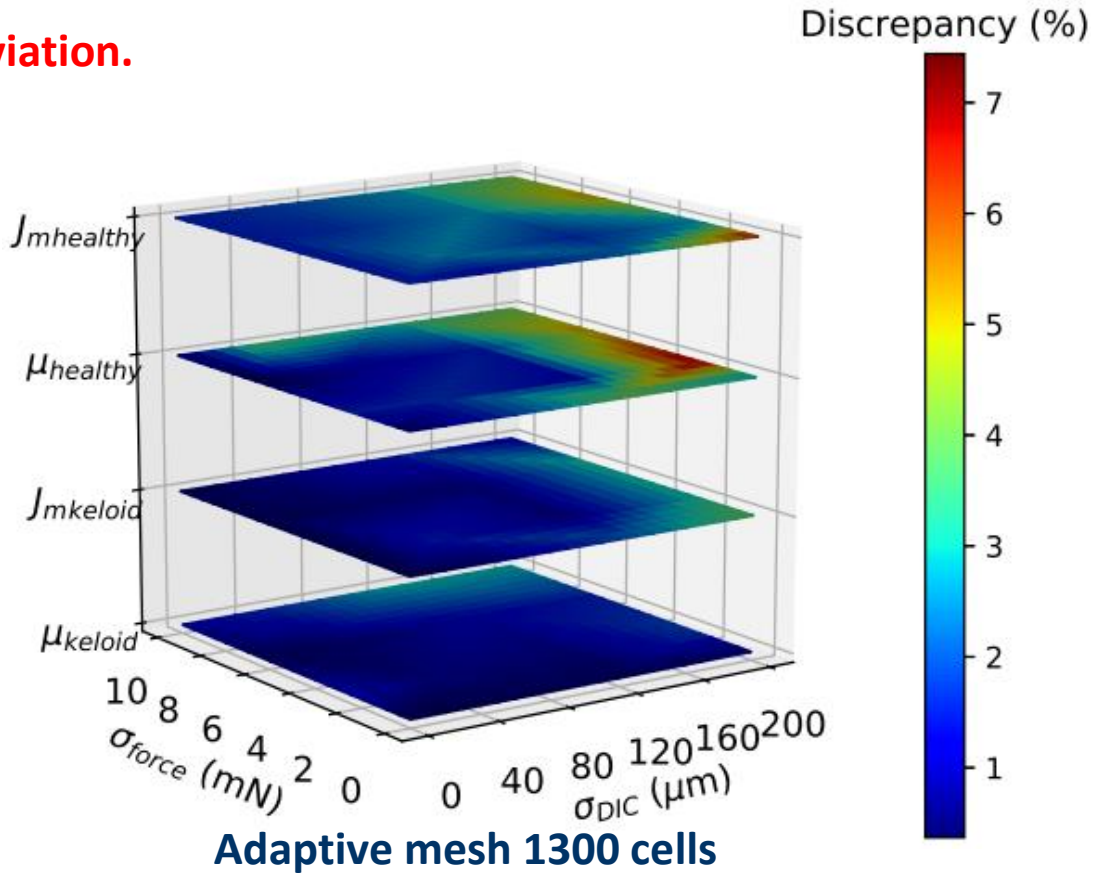

Adaptive mesh 1300 cells

Sensitivity analysis

- Discretization error.
- Measurement noises standard deviation.
- Number of DIC frames.

$$\sigma_{DIC} = 200\ \mu m \quad \sigma_{force} = 20\ mN$$

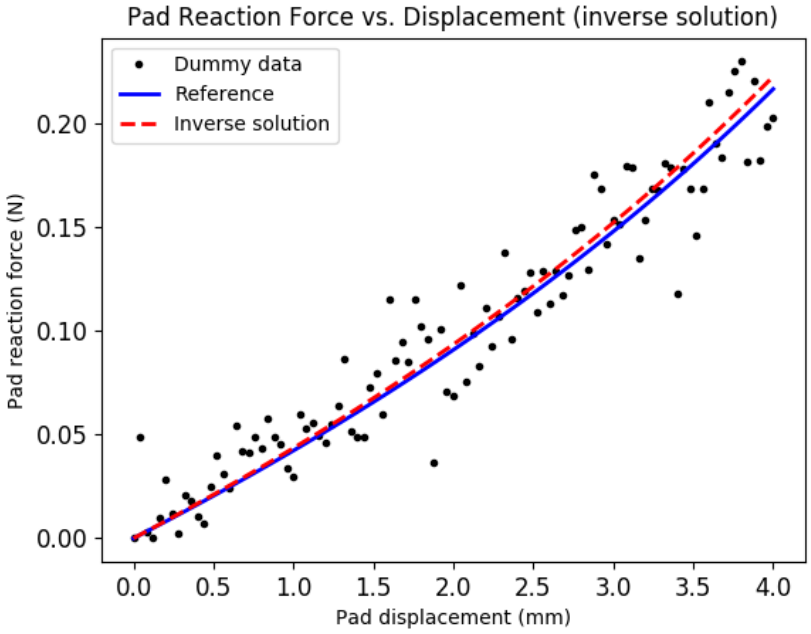

Weakly non-linear

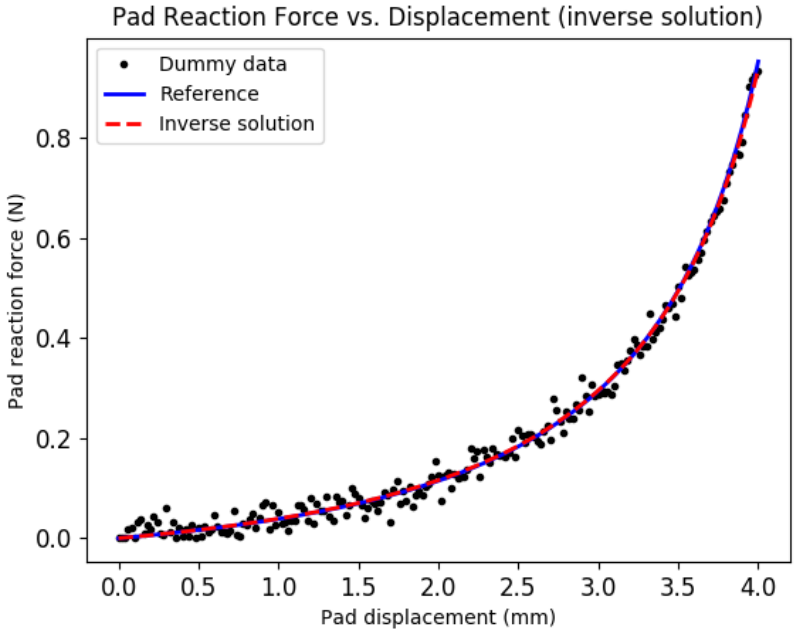

Highly non-linear

Sensitivity analysis

- Discretization error.
- Measurement noises standard deviation.
- Number of DIC frames.

$$\sigma_{DIC} = 200\ \mu m \quad \sigma_{force} = 20\ mN$$

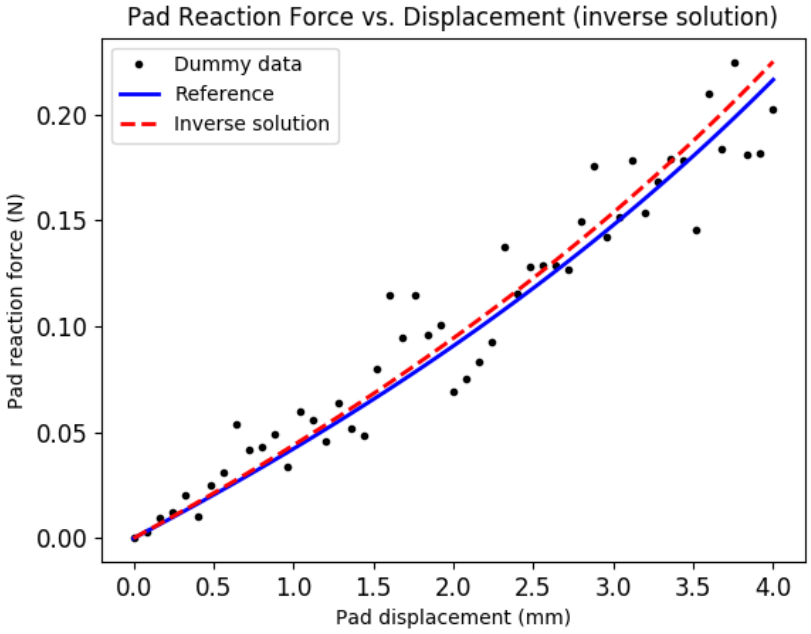

Weakly non-linear

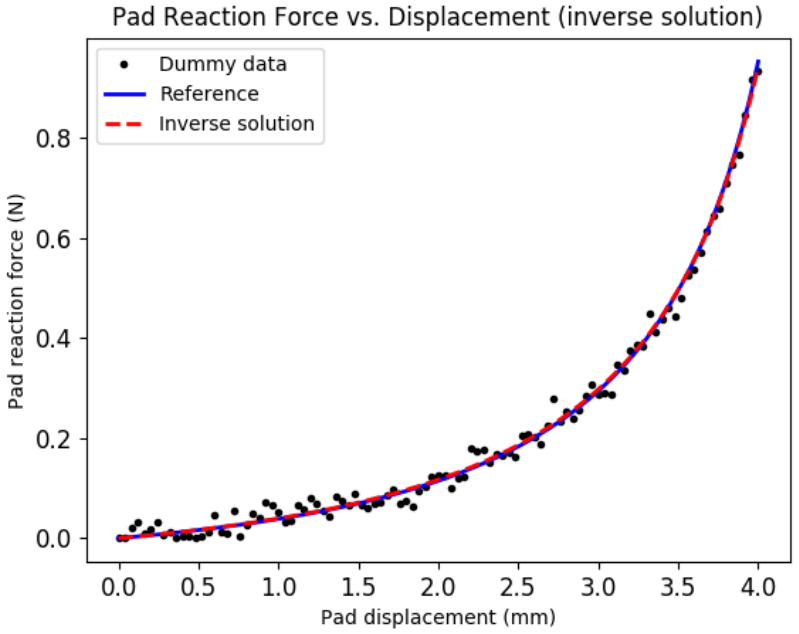

Highly non-linear

Sensitivity analysis

- Discretization error.
- Measurement noises standard deviation.
- Number of DIC frames.

$$\sigma_{DIC} = 200\ \mu m \quad \sigma_{force} = 20\ mN$$

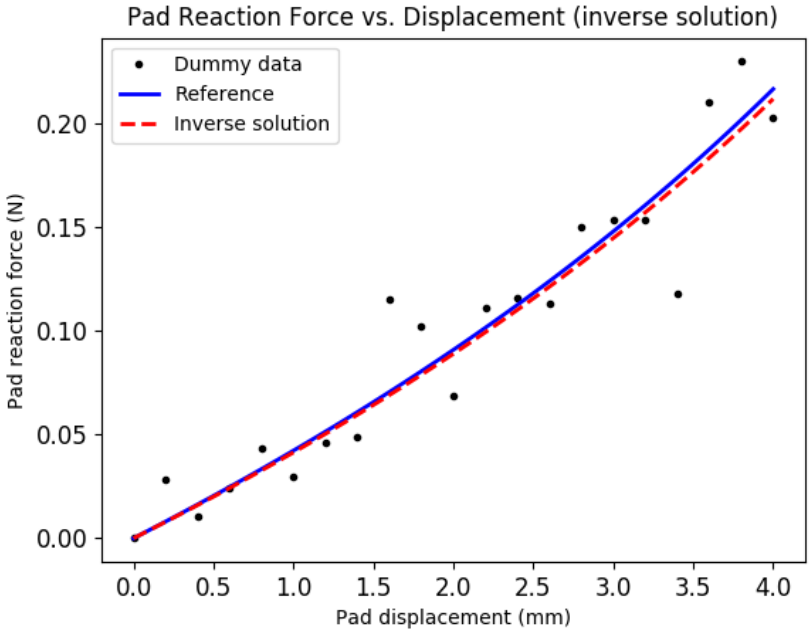

Weakly non-linear

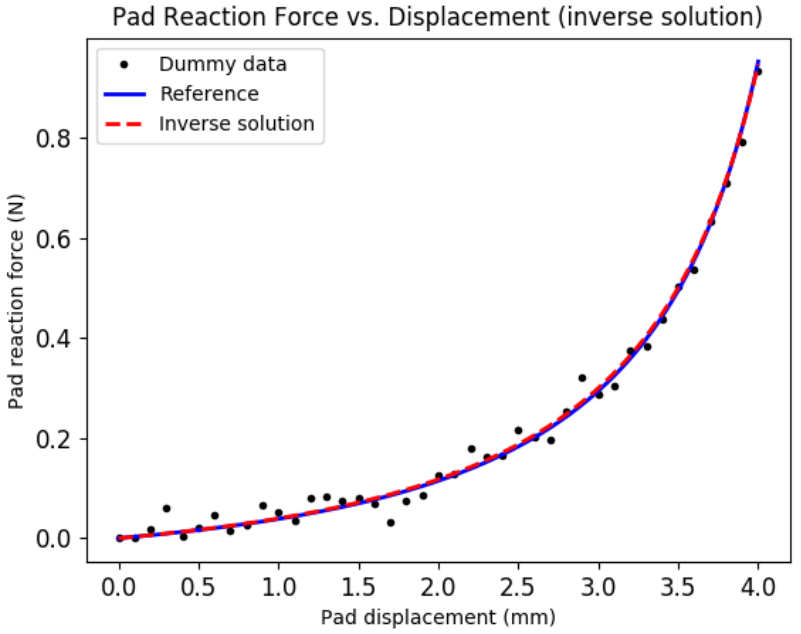

Highly non-linear

Sensitivity analysis

- Discretization error.
- Measurement noises standard deviation.
- Number of DIC frames.

$$\sigma_{DIC} = 200\ \mu m \quad \sigma_{force} = 20\ mN$$

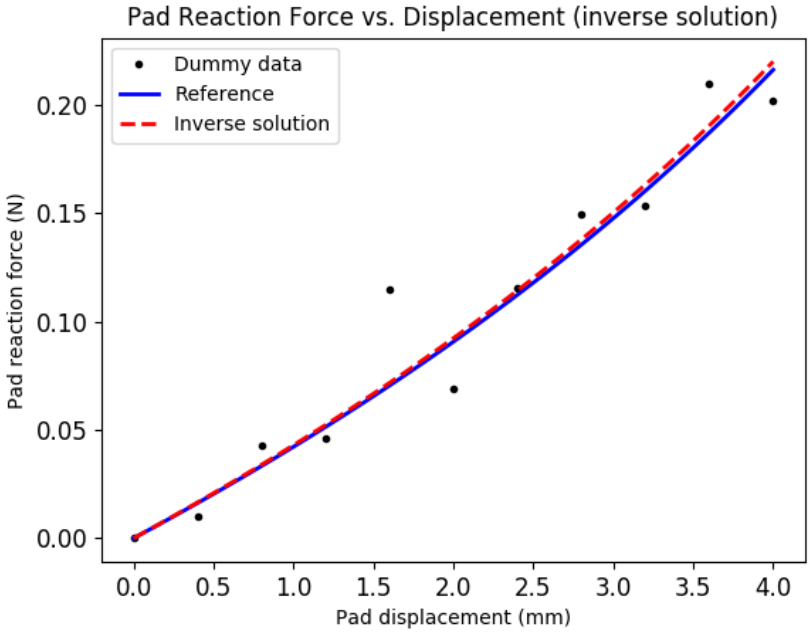

Weakly non-linear

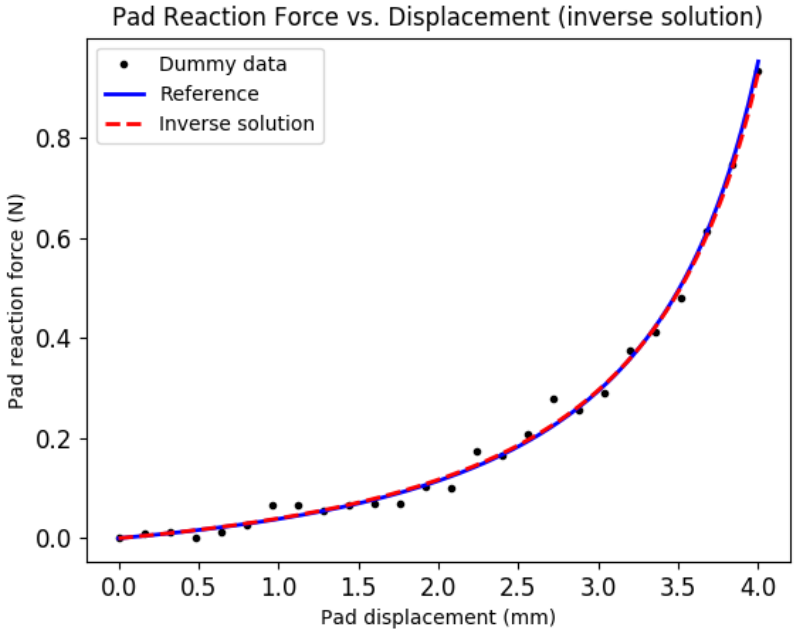

Highly non-linear

Sensitivity analysis

- Discretization error.
- Measurement noises standard deviation.
- Number of DIC frames.

$$\sigma_{DIC} = 200\ \mu m \quad \sigma_{force} = 20\ mN$$

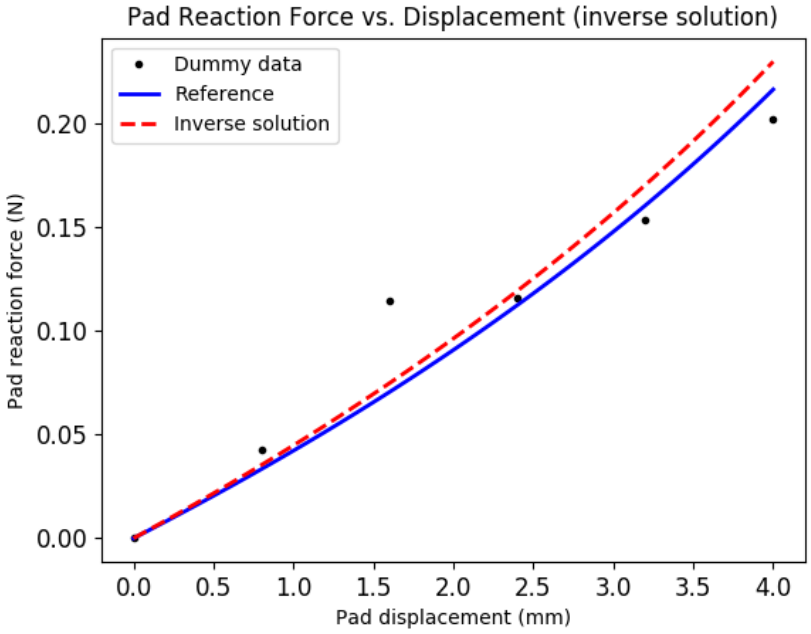

Weakly non-linear

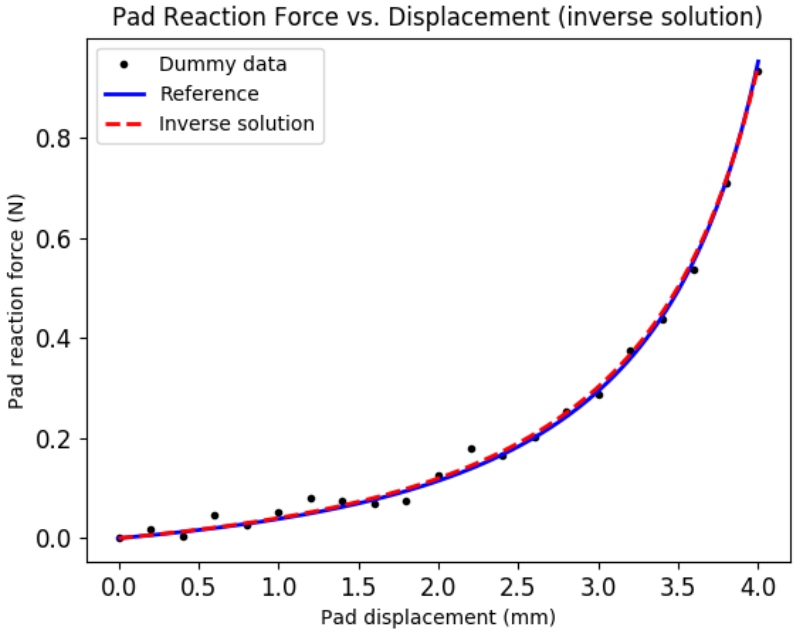

Highly non-linear

Sensitivity analysis

- Discretization error.
- Measurement noises standard deviation.
- Number of DIC frames.

$$\sigma_{DIC} = 200\ \mu m \quad \sigma_{force} = 20\ mN$$

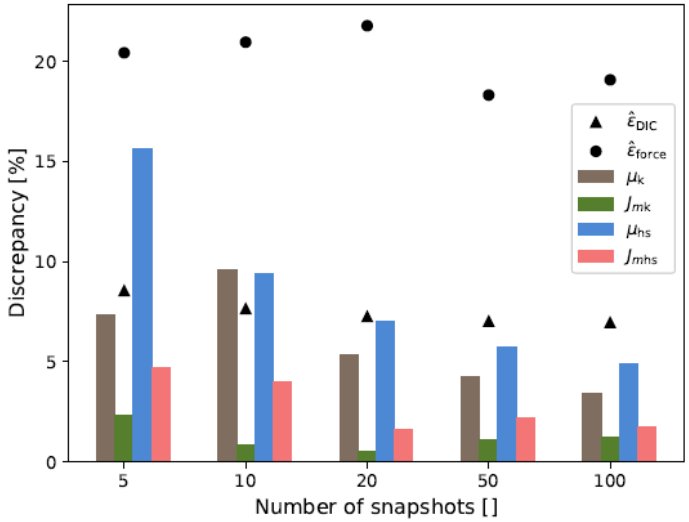

Weakly non-linear

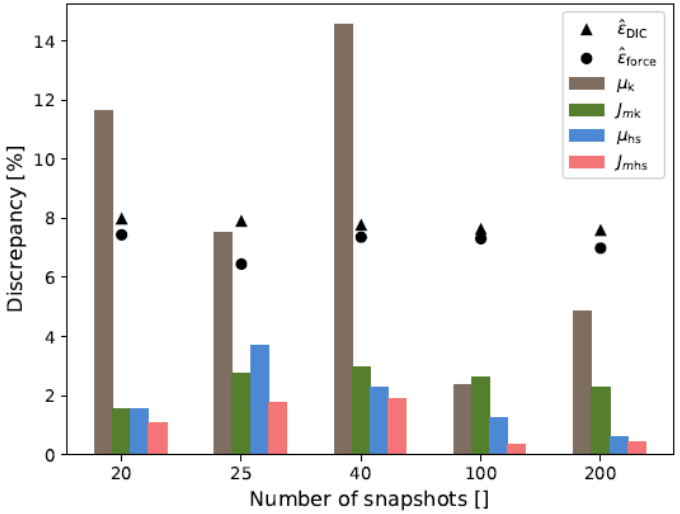

Highly non-linear

Application to keloid scar surrounded by healthy skin

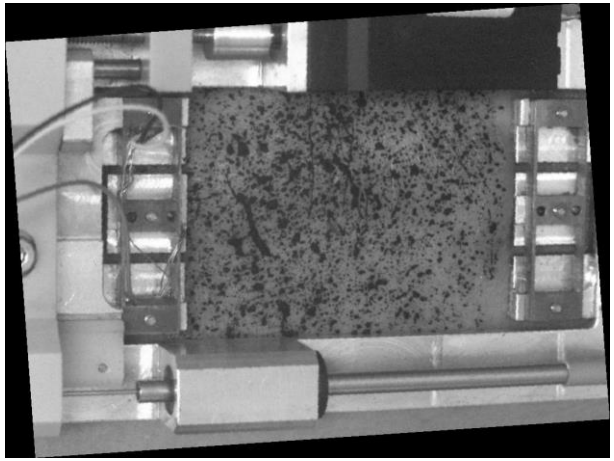

Keloid + surrounding healthy-skin

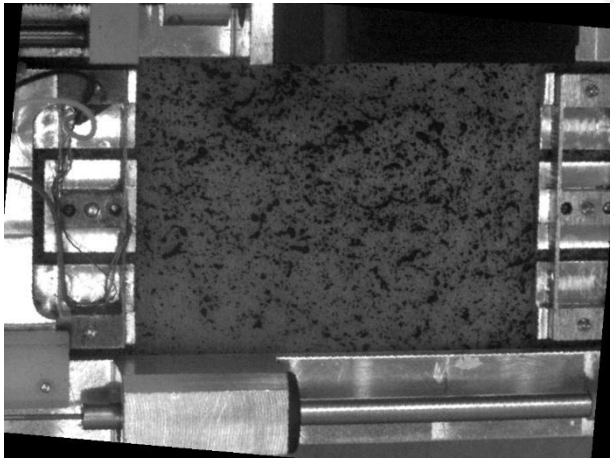

Healthy-skin (Colateral test)

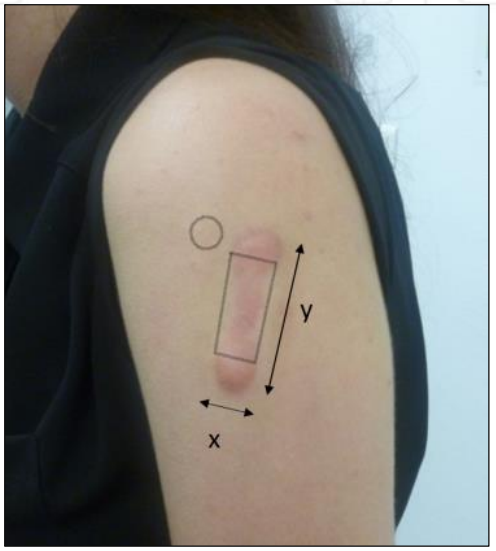

Butterfly-shaped keloid
(x=15mm, y=47mm)
(Chambert et al., 2019)

Neohookean **model**
2 parameters (healthy skin) + 2 parameters (keloid)
(Sutula et al., submitted)

Application to keloid scar surrounded by healthy skin

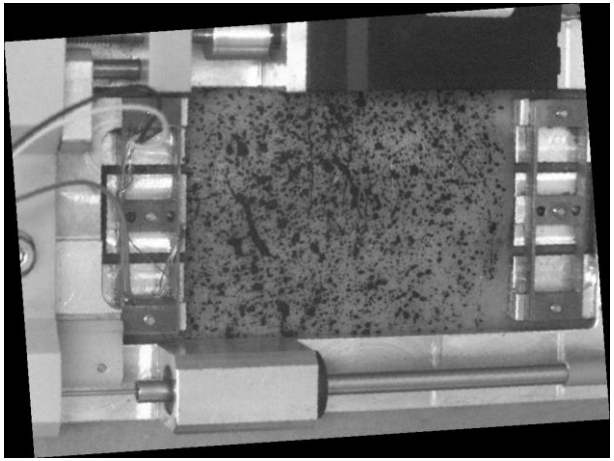

Keloid + surrounding healthy skin

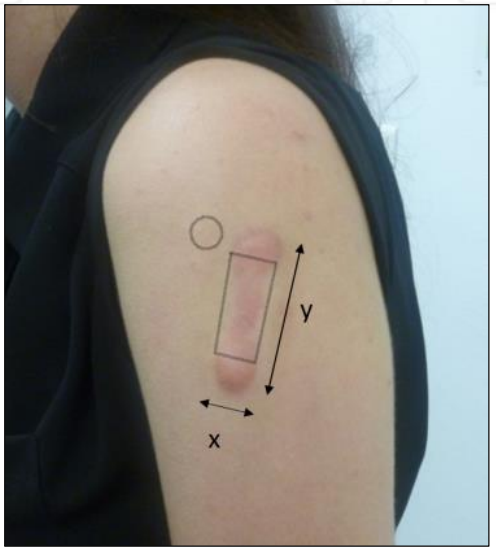

Butterfly-shaped keloid (x=15mm, y=47mm) (Chambert et al., 2019)

***Gent* model**

4 parameters (keloid + healthy-skin)

Application to keloid scar surrounded by healthy skin

Measurement uncertainty quantification

7.8 mN < 10 mN

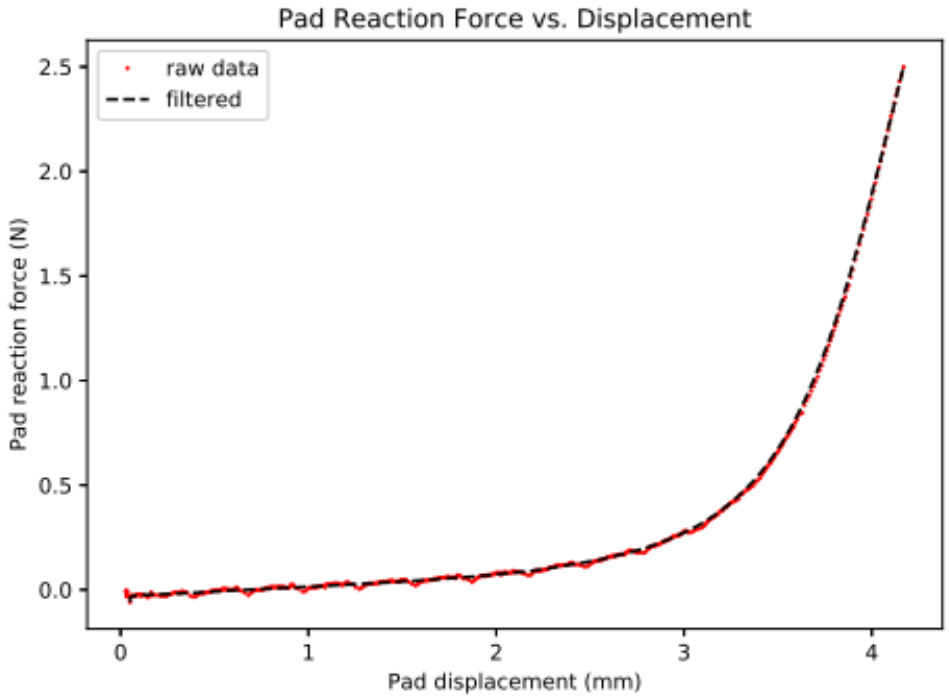

Data filtering with Moving-Average method

Application to keloid scar surrounded by healthy skin

Measurement uncertainty quantification

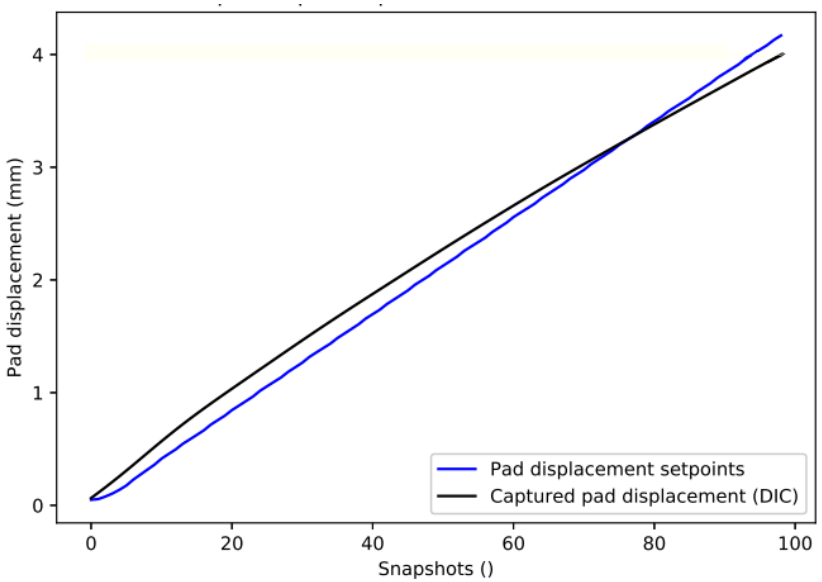

Captured pad displacement with DIC

128 µm < 160 µm

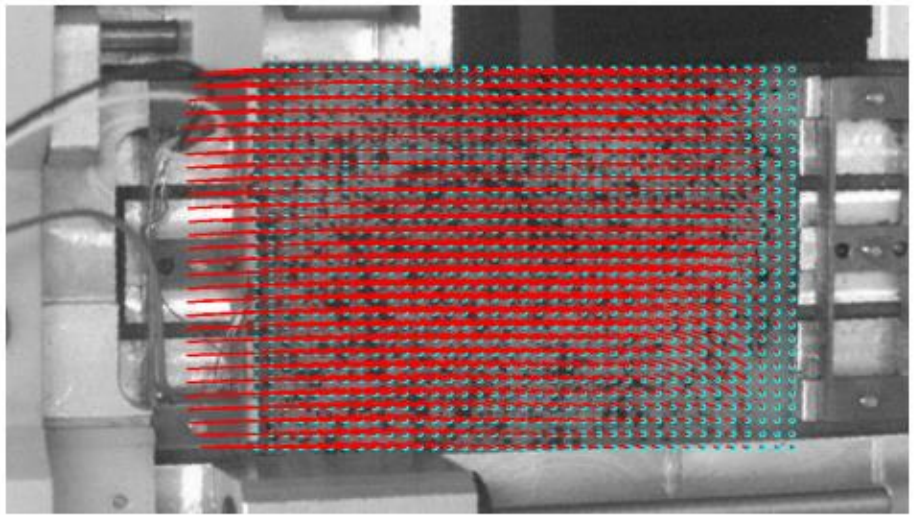

DIC with pyDIC library

https://github.com/ladisk/pyDIC

Application to keloid scar surrounded by healthy skin
Inverse identification

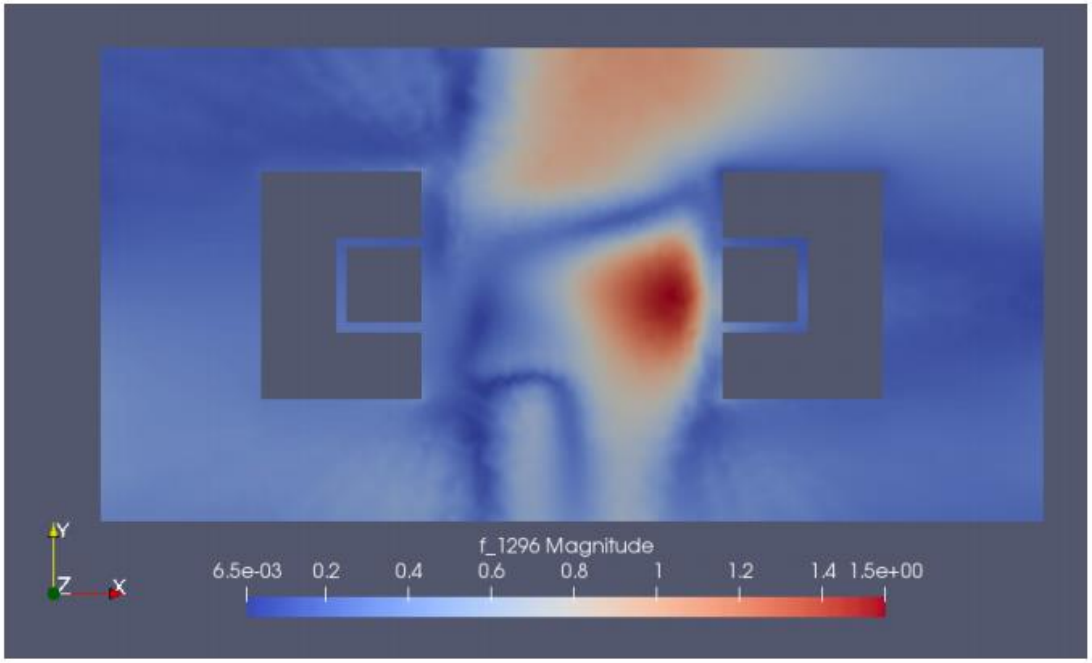

Discard between consistent (generated) and the experimental displacement fields

Application to keloid scar surrounded by healthy skin
Inverse identification

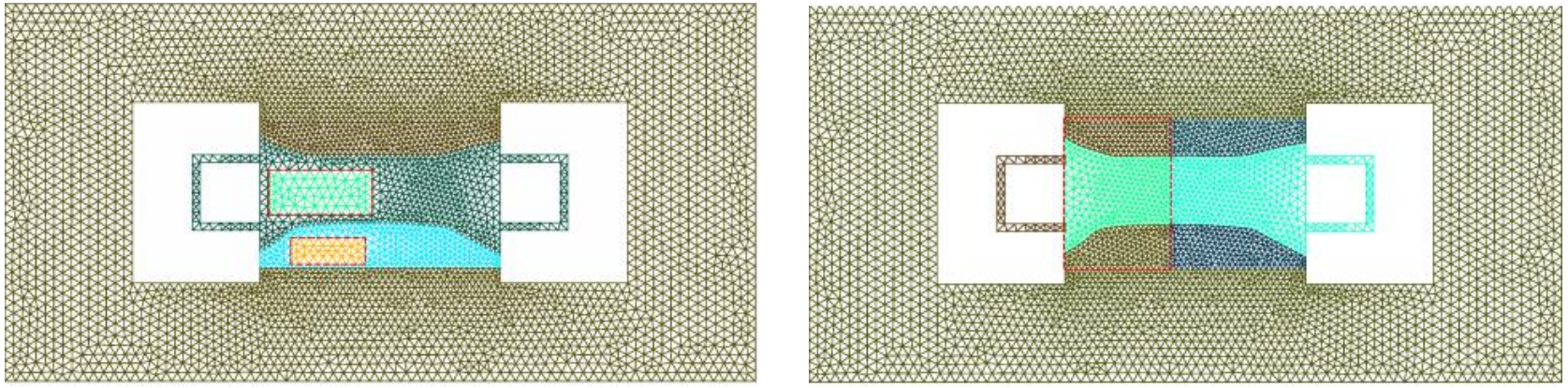

Splited and jointed optimization domains

Application to keloid scar surrounded by healthy skin

Inverse identification

Cost weights	ZOI configuration	Local optimum $\hat{\theta}$	ε_{force}	ε_{disp}	$\varepsilon_{force} + \varepsilon_{disp}$
Constant	Splited	$\mu_k = 9.26$ kPa $J_{mk} = 0.0154$ $\mu_{hs} = 6.98$ kPa $J_{mhs} = 0.169$	1.13%	4.92%	6.05%
Constant	Splited	$\mu_k = 8.11$ kPa $J_{mk} = 0.0142$ $\mu_{hs} = 5.58$ kPa $J_{mhs} = 0.163$	0.97%	5%	5.97%
Variable	Splited	$\mu_k = 6.686$ kPa $J_{mk} = 0.0127$ $\mu_{hs} = 4.404$ kPa $J_{mhs} = 0.153$	5.11%	5.17%	10.28%
Variable	Splited	$\mu_k = 7$ kPa $J_{mk} = 0.0124$ $\mu_{hs} = 4.43$ kPa $J_{mhs} = 0.157$	1.8%	5.1%	6.9%
Constant	Jointed	$\mu_k = 9.13$ kPa $J_{mk} = 0.0155$ $\mu_{hs} = 7.03$ kPa $J_{mhs} = 0.169$	1.09%	5.34%	6.43%
Constant	Jointed	$\mu_k = 8.35$ kPa $J_{mk} = 0.0142$ $\mu_{hs} = 5.99$ kPa $J_{mhs} = 0.167$	1.32%	5.4%	6.72%
Variable	Jointed	$\mu_k = 8.82$ kPa $J_{mk} = 0.0168$ $\mu_{hs} = 4.39$ kPa $J_{mhs} = 0.159$	2.3%	5.4%	7.7%

Summary of local optimums

Application to keloid scar surrounded by healthy skin

Inverse identification

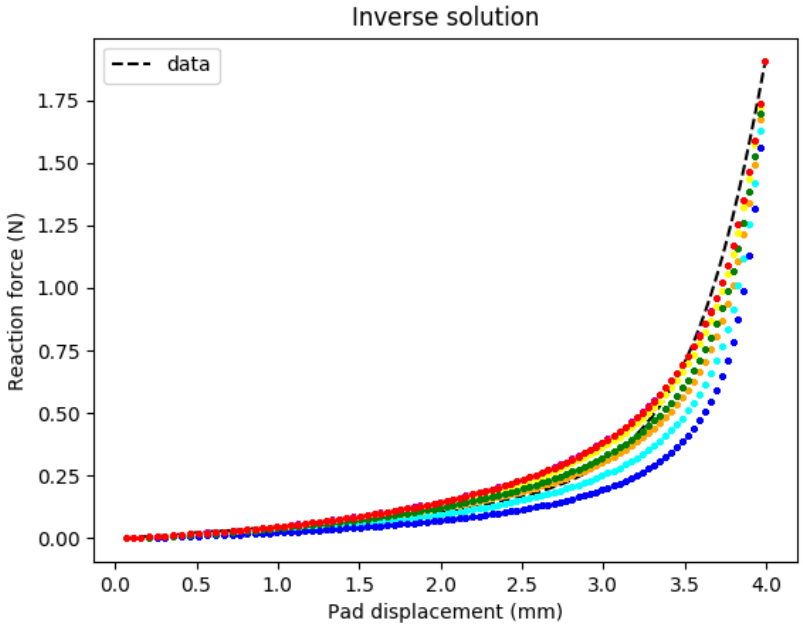

Inverse solution

Cost weights	ZOI configuration	Local optimum $\hat{\theta}$	ε_{force}	ε_{disp}	$\varepsilon_{force} + \varepsilon_{disp}$
Constant	Splited	$\mu_k = 9.26$ kPa $J_{mk} = 0.0154$ $\mu_{hs} = 6.98$ kPa $J_{mhs} = 0.169$	1.13%	4.92%	6.05%
Constant	Splited	$\mu_k = 8.11$ kPa $J_{mk} = 0.0142$ $\mu_{hs} = 5.58$ kPa $J_{mhs} = 0.163$	0.97%	5%	5.97%
Variable	Splited	$\mu_k = 6.686$ kPa $J_{mk} = 0.0127$ $\mu_{hs} = 4.404$ kPa $J_{mhs} = 0.153$	5.11%	5.17%	10.28%
Variable	Splited	$\mu_k = 7$ kPa $J_{mk} = 0.0124$ $\mu_{hs} = 4.43$ kPa $J_{mhs} = 0.157$	1.8%	5.1%	6.9%
Constant	Jointed	$\mu_k = 9.13$ kPa $J_{mk} = 0.0155$ $\mu_{hs} = 7.03$ kPa $J_{mhs} = 0.169$	1.09%	5.34%	6.43%
Constant	Jointed	$\mu_k = 8.35$ kPa $J_{mk} = 0.0142$ $\mu_{hs} = 5.99$ kPa $J_{mhs} = 0.167$	1.32%	5.4%	6.72%
Variable	Jointed	$\mu_k = 8.82$ kPa $J_{mk} = 0.0168$ $\mu_{hs} = 4.39$ kPa $J_{mhs} = 0.159$	2.3%	5.4%	7.7%

Summary of local optimums

Mechanical parameters identification of keloid and surrounding healthy skin using Digital Image Correlation measurements in vivo

Application to keloid scar surrounded by healthy skin

Inverse identification

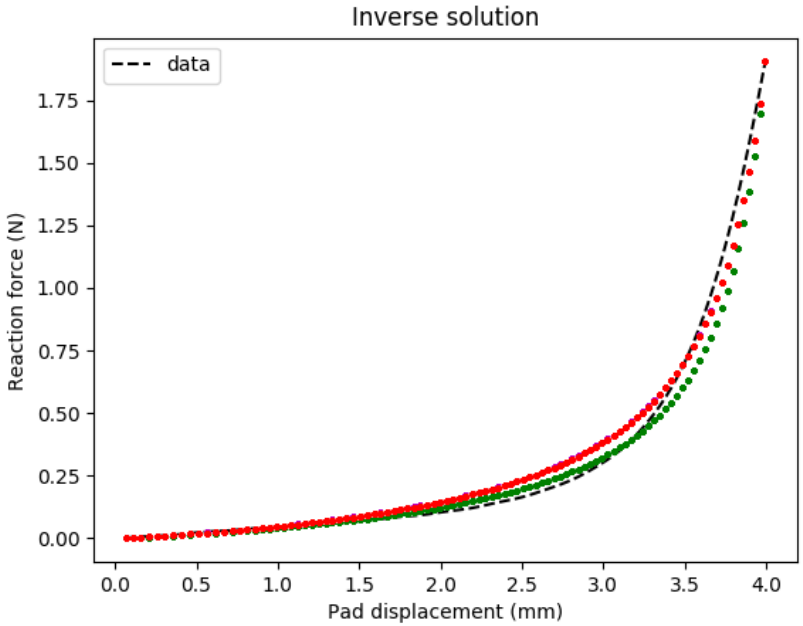

Inverse solution

Cost weights	ZOI configuration	Local optimum $\hat{\theta}$	ε_{force}	ε_{disp}	$\varepsilon_{force} + \varepsilon_{disp}$
Constant	Splited	$\mu_k = 9.26$ kPa $J_{mk} = 0.0154$ $\mu_{hs} = 6.98$ kPa $J_{mhs} = 0.169$	1.13%	4.92%	6.05%
Constant	Splited	$\mu_k = 8.11$ kPa $J_{mk} = 0.0142$ $\mu_{hs} = 5.58$ kPa $J_{mhs} = 0.163$	0.97%	5%	5.97%
Variable	Splited	$\mu_k = 6.686$ kPa $J_{mk} = 0.0127$ $\mu_{hs} = 4.404$ kPa $J_{mhs} = 0.153$	5.11%	5.17%	10.28%
Variable	Splited	$\mu_k = 7$ kPa $J_{mk} = 0.0124$ $\mu_{hs} = 4.43$ kPa $J_{mhs} = 0.157$	1.8%	5.1%	6.9%
Constant	Jointed	$\mu_k = 9.13$ kPa $J_{mk} = 0.0155$ $\mu_{hs} = 7.03$ kPa $J_{mhs} = 0.169$	1.09%	5.34%	6.43%
Constant	Jointed	$\mu_k = 8.35$ kPa $J_{mk} = 0.0142$ $\mu_{hs} = 5.99$ kPa $J_{mhs} = 0.167$	1.32%	5.4%	6.72%
Variable	Jointed	$\mu_k = 8.82$ kPa $J_{mk} = 0.0168$ $\mu_{hs} = 4.39$ kPa $J_{mhs} = 0.159$	2.3%	5.4%	7.7%

Summary of local optimums

Mechanical parameters identification of keloid and surrounding healthy skin using Digital Image Correlation measurements in vivo

Application to keloid scar surrounded by healthy skin

Inverse identification

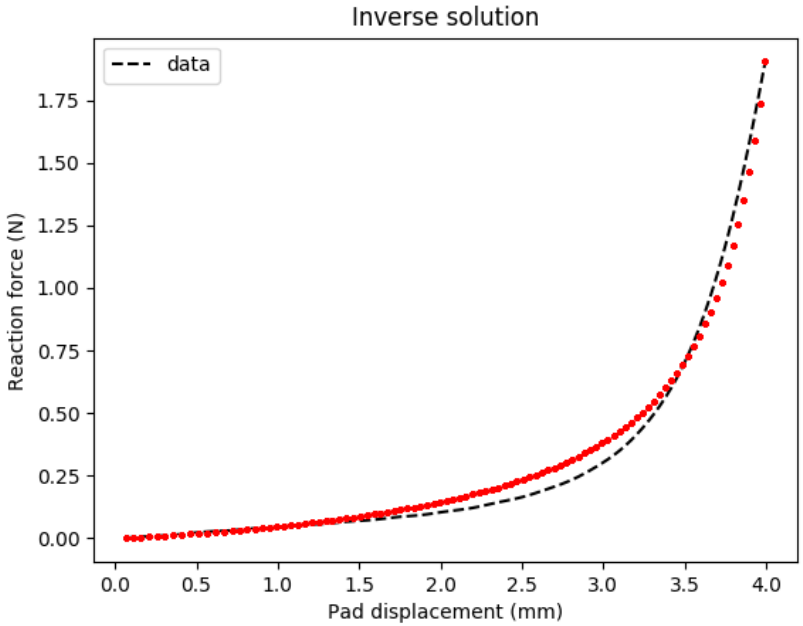

Inverse solution

Cost weights	ZOI configuration	Local optimum $\hat{\theta}$	ε_{force}	ε_{disp}	$\varepsilon_{force} + \varepsilon_{disp}$
Constant	Splited	$\mu_k = 9.26$ kPa $J_{mk} = 0.0154$ $\mu_{hs} = 6.98$ kPa $J_{mhs} = 0.169$	1.13%	4.92%	6.05%
Constant	Splited	$\mu_k = 8.11$ kPa $J_{mk} = 0.0142$ $\mu_{hs} = 5.58$ kPa $J_{mhs} = 0.163$	0.97%	5%	5.97%
Variable	Splited	$\mu_k = 6.686$ kPa $J_{mk} = 0.0127$ $\mu_{hs} = 4.404$ kPa $J_{mhs} = 0.153$	5.11%	5.17%	10.28%
Variable	Splited	$\mu_k = 7$ kPa $J_{mk} = 0.0124$ $\mu_{hs} = 4.43$ kPa $J_{mhs} = 0.157$	1.8%	5.1%	6.9%
Constant	Jointed	$\mu_k = 9.13$ kPa $J_{mk} = 0.0155$ $\mu_{hs} = 7.03$ kPa $J_{mhs} = 0.169$	1.09%	5.34%	6.43%
Constant	Jointed	$\mu_k = 8.35$ kPa $J_{mk} = 0.0142$ $\mu_{hs} = 5.99$ kPa $J_{mhs} = 0.167$	1.32%	5.4%	6.72%
Variable	Jointed	$\mu_k = 8.82$ kPa $J_{mk} = 0.0168$ $\mu_{hs} = 4.39$ kPa $J_{mhs} = 0.159$	2.3%	5.4%	7.7%

Summary of local optimums

Mechanical parameters identification of keloid and surrounding healthy skin using Digital Image Correlation measurements in vivo

Conclusion and perspectives

A primary material parameter set of keloid/healthy-skin has been identified by taking into account measurement noise admissibility criteria.

Conclusion and perspectives

A primary material parameter set of keloid/healthy-skin has been identified by taking into account measurement noise admissibility criteria.

- **Develop a full 3D or pseudo-3D FE model.**
- **Model selection.**
- **Use stochastic method - Bayesian inference- to identify a global optimum. (?)**
- **Identify earlobe keloid parameters through suction test**

Thank you for your attention !

Questions ?